

ATLAS
HEC-Note- 124
March 2002

Preshaper for the Hadron End-Cap Calorimeter

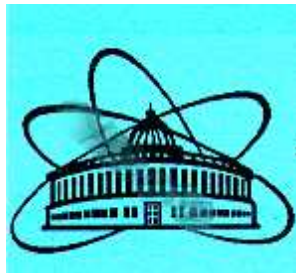
Production Readiness Review

E.Ladygin

Joint Institute for Nuclear Research, Dubna, Russia

W.-D.Cwienk, L. Kurchaninov, P.Strizenec

Max-Planck-Institut für Physik, Munich, Germany



Documentation for the preshaper Production Readiness Review is organized in the following way:

- | | |
|---|--|
| 1. The HEC preshaper | <i>Presented by:</i>
<i>L.Kurchaninov</i> |
| 1.1 Introduction | |
| 1.2 Preshaper version 0 | |
| 1.3 Technical specifications | |
| 2. Design and simulations | <i>E.Ladygin</i> |
| 2.1 Scheme of the preshaper | |
| 2.2 Results of simulations | |
| 2.3 Power consumption | |
| 3. Laboratory tests | <i>E.Ladygin</i> |
| 3.1 Measuring setup | |
| 3.2 Signal shape analysis | |
| 3.3 Rise time compensation | |
| 3.4 Gain and gain uniformity | |
| 3.5 Noise | |
| 3.6 Preshaper performance on FEB0 | |
| 4. Test beam results | <i>L.Kurchaninov</i> |
| 4.1 Test-beam electronics | |
| 4.2 Preshaper characteristics | |
| 4.3 Noise of HEC chain | |
| 4.4 Physical waveform | |
| 5. Radiation test | <i>E.Ladygin</i> |
| 6. Burn-in test and failure rate | <i>L.Kurchaninov</i> |
| 7. QC procedure | <i>E.Ladygin</i> |
| 8. Production plans | <i>L.Kurchaninov</i> |
| 9. References | |
| 10. Appendix A: HEC electronic chain | |
| 11. Appendix B: Components list of preshaper | |
| 12. Appendix C: LSB output amplitudes | |

1. HEC Preshaper: Requirements and Specifications

1.1 INTRODUCTION

Signals from the ATLAS Liquid Argon (LAr) calorimeter are processed by front-end electronics, which has unique architecture for all sub detectors [1]. At the same time the HEC is equipped by cold preamplifiers instead of warm „0T“ amplifiers that are used for electromagnetic (EMC) and forward calorimeters. The transfer function of GaAs front-end chips differs from that of 0T, so an additional circuit is required to match the input range of the shaper. The place in the front-end board (FEB) reserved for the warm preamplifiers can be used for this circuit, which we refer to as a „**preshaper**“.

The preshaper has been proposed and discussed during HEC Electronics Meeting in February 1997 [2] with the following functions:

- Inversion of the signal polarity
- Amplification with factor 4 (or close to that, depending on the preamplifier gain) for the front HEC module and factor 8 for the rear one;
- Compensation of the preamplifier rise time by using standard pole-zero cancellation method.

The requirements to the preshaper have been formulated for the first time in the HEC Note-073 [3]. The preshaper version 0 [4] have been developed and produced on the basis of those requirements. Afterwards, in the end of 1998, the HEC cold cables have been measured and the signal distortion was parameterized [5], that led to some corrections to the preshaper gain and time constants. These corrections have been applied in the next version 1.

1.2 PRESHAPER VERSION 0

In the beginning of 1999 about 150 hybrids of version 0 have been produced. These hybrids have been tested in laboratory conditions and used in the HEC test beam setup during 1999-2001 beam periods. Test-beam measurements showed that the version 0 does not satisfy to all requirements.

Design review of preshaper version 0 held in May 2000. The preshaper design has been accepted without major modifications, but Reviewers did few comments:

- check a violation of accuracy on E_t with peaking time dispersion
- provide the official radiation figures
- simulate the safeguard against oscillation, show Bode plots
- study stability with lower output resistor to improve linearity and uniformity against the shaper input impedance variation
- show gain and peaking time variation with beta (β) of transistors and temperature
- change the integration time constant to get the peaking time slightly below 50ns
- simulate the power supply rejection ratio
- explain the large gain and peaking time variation on beam setup

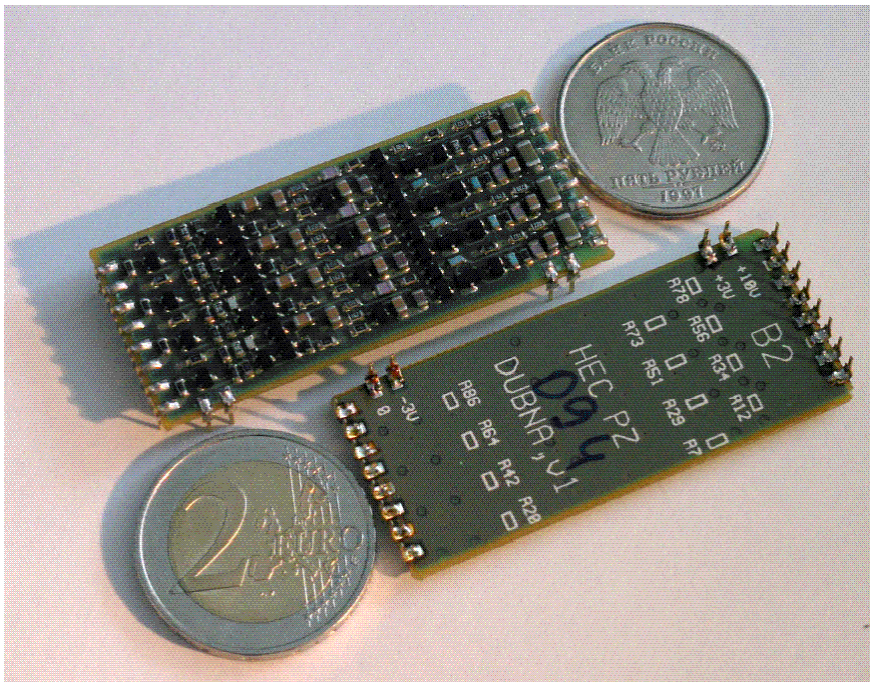
- specify the noise performance
- measure the preshaper on the populated FEB0
- further study of the parameters extraction in Quality Control procedure

Additional points should be discussed and clarified:

- series shaper characteristics
- LSB switch point
- output range requirements
- gamma irradiation on production hybrids
- Burn-in of 100% hybrids
- pins part number

The version 1 of preshaper has been designed and produced in 2001. New preshaper has shorter integration time constant in order to achieve the required peaking time of 50ns, standard pins and better safeguard against oscillations.

Hybrids are made by SMD technology as small printed circuit board on G10 material of 1mm thickness and produced by Moscow Institute for Precision Mechanics and Computing Techniques. Below the photo of preshaper is given. Information about name and type of a hybrid is marked at the bottom side. In future it will have the serial number of hybrid too.



1.3 TECHNICAL SPECIFICATIONS

All the specification requirements to the preshaper are determined either by the HEC cold electronics or by the shaper characteristics and the front-end board (FEB) layout.

The HEC calorimeter consists of 7 longitudinal blocks, grouped to 4 longitudinal readout segments. Figure 1 schematically shows the HEC segmentation. After the preamplifying and summing boards (PSB) the signals from 4 segments go to 4 successive channels of the preshaper, the first three of them will be used to form the trigger tower. The scheme of the signals summing is presented in Figure 2.

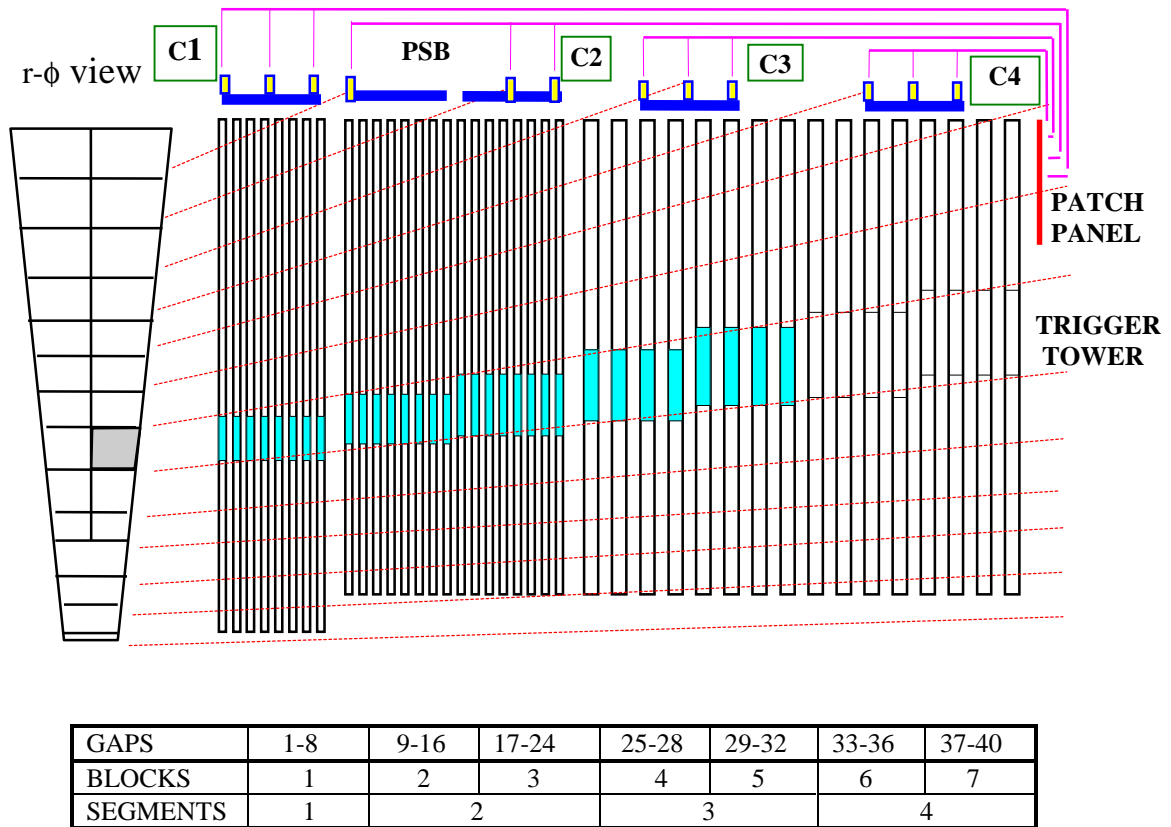


Figure 1: Scheme of the HEC module segmentation.
 The trigger signal is formed by the first 32 double gaps.

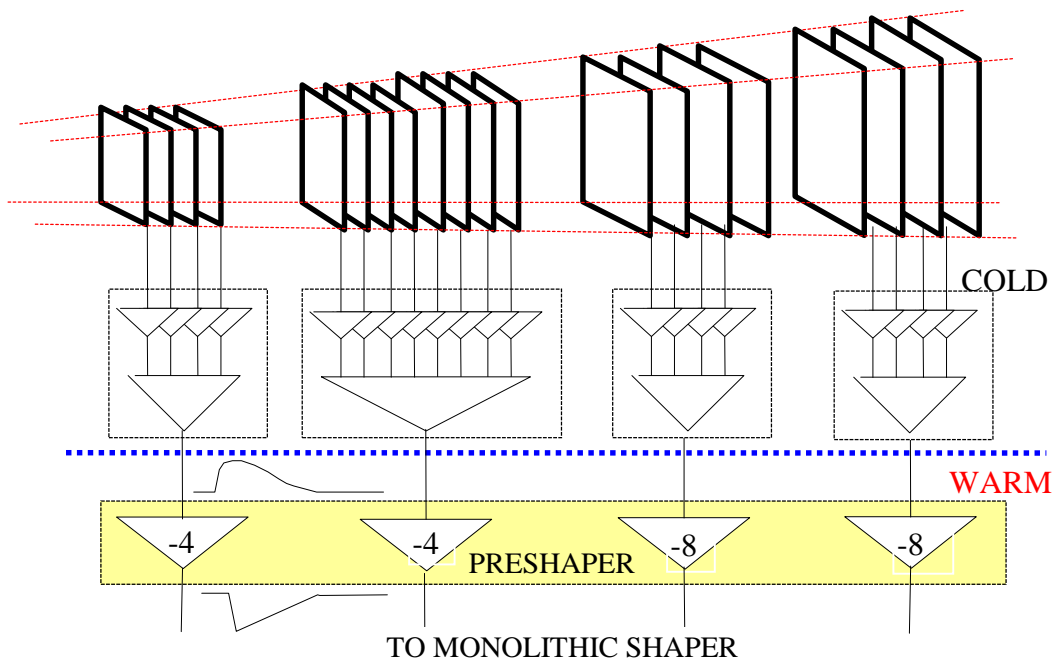


Figure 2: The HEC summation scheme. The first three preshaper outputs are used for the trigger sum.

Different HEC readout towers have different capacitances so that signals in different channels have different rise time due to the integration on the input impedance of the preamplifier. This rise time can be calculated using the simple formula:

$$\tau_{pa} = R_a \cdot (C_d + C_a)$$

R_a is the preamplifier input impedance (typically 50Ω in cold and 70Ω at room temperature, varying from chip to chip), C_d is the detector capacitance, from 24pF to 410pF and C_a is the preamplifier input capacitance, typically 50pF at LAr temperatures.

The preshaper zero time constant has to be adjusted to the preamplifier rise time. We decided to make this adjustment for all different HEC channels that brings us to 14 different time constants. Since the preshapers are placed on two sides of the FEB – top and bottom, which are not symmetrical, the total number of types is 28.

So the first requirements are:

SR1: 4 channels per hybrid, corresponding to 4 longitudinal HEC segments

SR2: 14 different time constants according to HEC capacitances, 28 different types of hybrids

The HEC segments have different sampling fractions, twice smaller in the rear part. In order to produce signals, proportional to the energy deposition, the last two preshaper channels have twice-higher gain. The absolute value of the gain is determined by the preamplifier transfer function and, from other side, by the shaper working range. So, the gain has to be:

SR3: Gain (in amplitude) is 4.0 for channels, processing front module and 8.0 - rear one. The uniformity is better than $\pm 2.5\%$ [6]

SR4: Inversion of the signal polarity. Input signals are positive, output are negative

Since the cables used in the electronics chain have 50Ω impedance, so:

SR5: The input impedance of the preshaper is 50Ω

The shapers designed for the Liquid Argon Detectors have the shaping time constant of $\sim 14\text{ns}$ [7]. In order to reach a peaking time of 50ns, an additional integration time constant has to be introduced in the preshaper. In [3] this time constant was calculated as 26ns, and afterwards, taking into account the cable effect, it was re-estimated as 14ns [5]. Since the signals from 3 successive channels go to the trigger summation, they have to be equalized in peaking time. So:

SR6: The peaking time for ionization signal is 50ns and uniformity is better than $\pm 2.5\text{ns}$

Mainly the preamplifiers determine the total noise in the HEC chain, and it can not be increased significantly by the preshaper:

SR7: The contribution to the equivalent noise current is less than 5% of the preamplifier noise

The preshaper are plugged in the place of 0T preamplifier on the FEB. Obvious requirements are mechanical and electrical compatibility:

SR8: The same pin-out as 0T circuit: 20 pins with 2.54mm distance, 5mm length

SR9: The same dimensions as 0T circuit: 53x23 mm² with board thickness 1.0±0.1mm. The height of components is not more than 1.5mm (when mounted on the FEB the hybrid's height must not exceed 5mm)

SR10: Operating voltages: +10V±10%, +3V±10%, -3V±10%

SR11: Power consumption less than 50mW/channel

The preshaper has not to introduce the non-linearity to the chain. The reasonable requirement is (typical for all components):

SR12: Integral non-linearity for negative output signal up to 4 V loaded by 50Ω resistor - better than 1%

All electronic circuits in ATLAS have to satisfy the requirements of RHA [8,9]. Using the radiation levels in HEC Front End Crate region and safety factors, we have:

SR13: Ionizing radiation hardness: 350Gy in 10 years

SR14: Neutron radiation hardness: 3.2·10¹² n/cm² in 10 years

SR15: Failure rate less than 0.5% per year over 10 years

2. Design and SPICE Simulations

2.1 SCHEME OF THE PRESHAPER

The functional diagram of the preshaper is shown in Figure 3. It consists of two stages. The first stage provides the required amplification, inversion of the signal and additional integration while the second one is the standard pole-zero cancellation scheme.

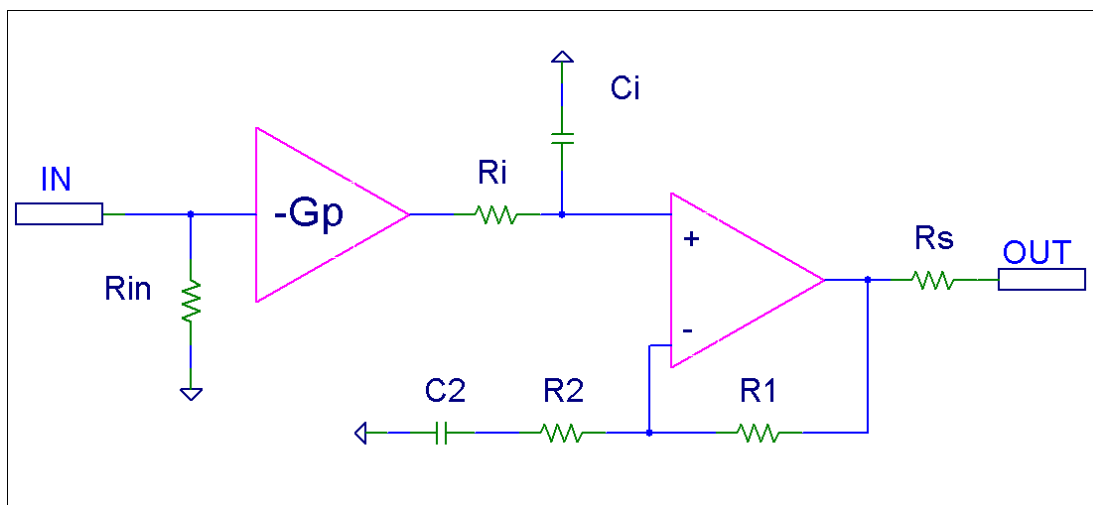


Figure 3: Functional diagram of the preshaper.

The transfer function of the circuit in Laplace domain can be written as:

$$H_p(s) = -\frac{G_p \cdot Rinsh}{(Rs + Rinsh)} \cdot \frac{1 + s \cdot C2 \cdot (R1 + R2)}{(1 + s \cdot C2 \cdot R2) \cdot (1 + s \cdot Ci \cdot Ri)}$$

where $Rinsh$ is the input impedance of the following shaper, which is 50 Ohms.

The zero time constant is determined by $C2 \cdot (R1 + R2)$. $R2$ and $C2$ are selected as unchangeable, and $R1$ is used to adjust the time constant. $R1$ value can be determined from the equality:

$$\tau_{pz} = \tau_{pa} \quad \text{or} \quad C2 \cdot (R1 + R2) = (Cd + Ca) \cdot Rin$$

Using detector capacitance Cd for different HEC channels, the values of τ_{pz} have been calculated. These values and amplification of channels are given in table 1. The amplification for step response has been selected as -6 and -12 instead -5.4 and -10.8 [5] because of the shaper gain is 0.83 instead of expected 1.0.

#type	τ_{pz} [ns]				Gp [V/V]			
	Ch 1	Ch 2	Ch 3	Ch 4	Ch 1	Ch 2	Ch 3	Ch 4
T1	13.69	9.79	3.67	3.67	-6	-6	-12	-12
T2	13.69	13.69	8.23	3.67	-6	-6	-12	-12
T3	18.76	12.52	13.69	13.69	-6	-6	-12	-12
T4	16.03	18.76	12.52	14.86	-6	-6	-12	-12
T5	13.69	16.03	18.76	21.88	-6	-6	-12	-12
T6	11.35	12.52	16.03	17.20	-6	-6	-12	-12
T7	9.79	10.57	12.52	14.86	-6	-6	-12	-12
T8	8.23	9.01	11.35	12.52	-6	-6	-12	-12
T9	7.06	7.84	9.01	10.57	-6	-6	-12	-12
T10	6.28	7.06	8.23	9.01	-6	-6	-12	-12
T11	13.69	16.03	18.76	21.88	-6	-6	-12	-12
T12	9.79	11.35	13.69	14.86	-6	-6	-12	-12
T13	7.06	5.89	10.57	11.35	-6	-6	-12	-12
T14	3.67	3.67	3.67	5.54	-6	-6	-12	-12
B1	3.67	3.67	9.79	13.69	-12	-12	-6	-6
B2	3.67	8.23	13.69	13.69	-12	-12	-6	-6
B3	13.69	13.69	12.52	18.76	-12	-12	-6	-6
B4	14.86	12.52	18.76	16.03	-12	-12	-6	-6
B5	21.88	18.76	16.03	13.69	-12	-12	-6	-6
B6	17.20	16.03	12.52	11.35	-12	-12	-6	-6
B7	14.86	12.52	10.57	9.79	-12	-12	-6	-6
B8	12.52	11.35	9.01	8.23	-12	-12	-6	-6
B9	10.57	9.01	7.84	7.06	-12	-12	-6	-6
B10	9.01	8.23	7.06	6.28	-12	-12	-6	-6
B11	21.88	18.76	16.03	13.69	-12	-12	-6	-6
B12	14.86	13.69	11.35	9.79	-12	-12	-6	-6
B13	11.35	10.57	5.89	7.06	-12	-12	-6	-6
B14	5.54	3.67	3.67	3.67	-12	-12	-6	-6

Table 1: Zero time constant and gain for different types of preshapers.

The circuit is made by using the microwave bipolar transistors since the usage of operational amplifiers is problematic with respect to noise. The schematic diagram is shown in Figure 4 and the layout is presented in Figure 5.

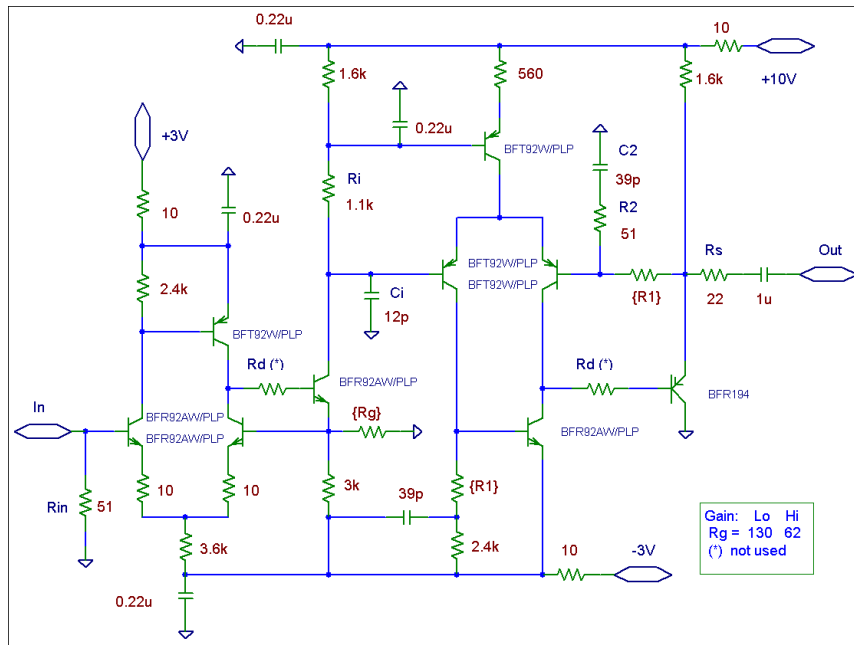
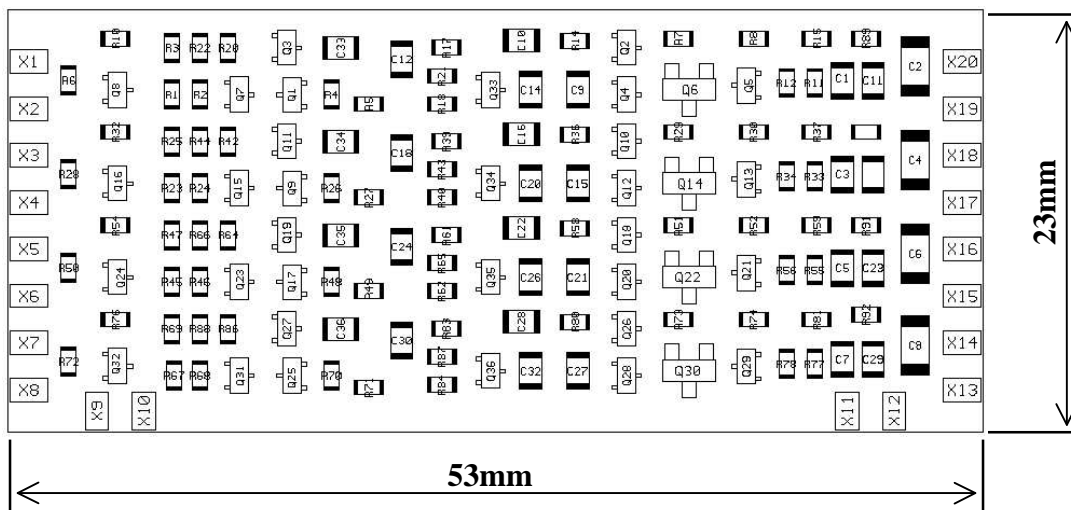


Figure 4: Schematic diagram of one preshaper channel.



Pin number	Pin name
X1, X3, X5, X7	input
X19, X17, X15, X13	output
X2, X4, X6, X8, X9, X14, X16, X18, X29	ground
X10	Vss (-3V)
X11	Vcc (+3V)
X12	Vdd (+10V)

Figure 5: Layout of the preshaper(top view) and pins assignment.

2.2 RESULTS OF SIMULATIONS

Important preshaper characteristics are the transfer function, noise, stability against oscillations and temperature performance. They have been simulated by SPICE using PHILIPS models of transistors. Figure 6 shows the triangle response of the preshaper. For comparison the response of the ideal Laplace circuit is also given. Rise time of the real preshaper is longer, which is explained by the limited frequency band of the components.

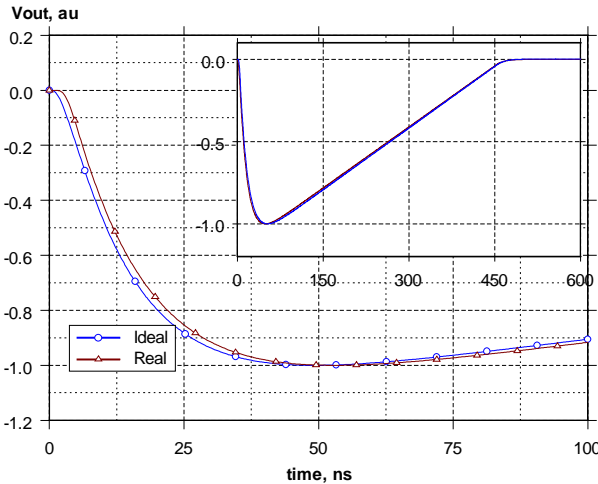


Figure 6: Simulated triangle response of the real and ideal LAPLACE preshaper for $C_d=200\text{pF}$.

The simulated peaking time of the preshaper with full HEC chain model and ideal shaper is equal to 50.3ns (Figure 7), that is in a good agreement with **SR6**.

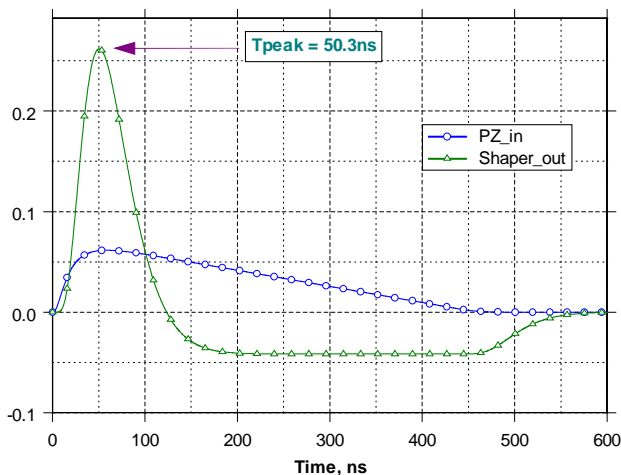


Figure 7: Simulated triangle response of the real preshaper and ideal $13.7\text{ns } RC^2\text{-CR}$ shaper for the case of $C_d=200\text{pF}$.

So as the schematic is made of discrete components the dispersion of gain and peaking time variations against the tolerance of components (nominal of resistor and capacitor, beta of transistors) has been simulated (Figure 8). RMS of the gain variation is less than 1%, and peaking time is less than 0.7ns. Simulated variation of the gain and peaking time in temperature range of 10÷50 °C is negligible.

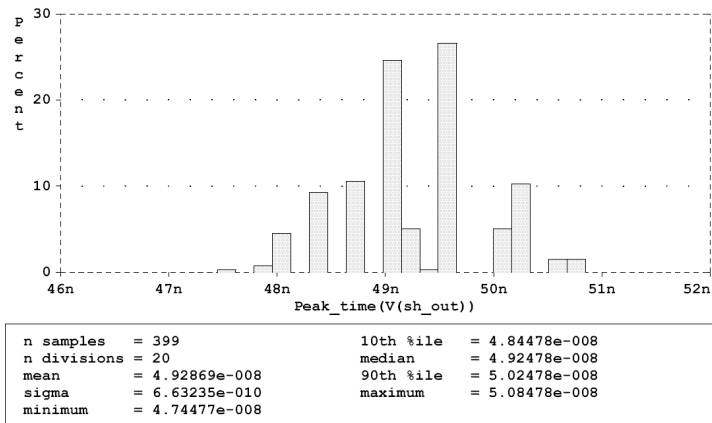
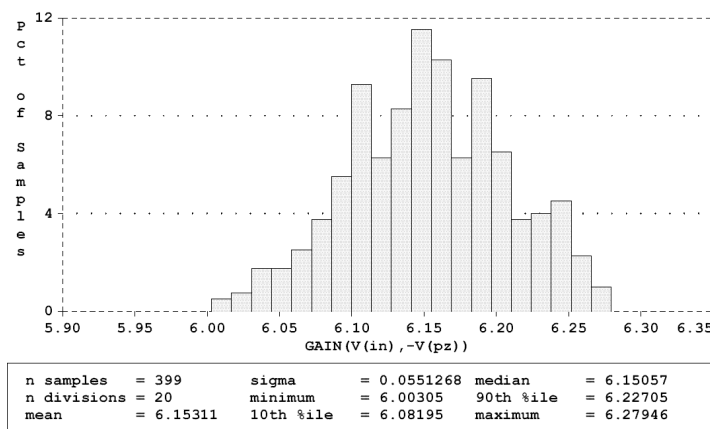


Figure 8: Peaking time and gain distributions for the component tolerance of resistor 1%, capacitor 5%, transistor beta $\pm 50\%$.



The simulated output noise is in the range of 54÷103 μ V for the required Cd range of 24÷410pF. The typical equivalent noise current of the preamplifier with $Cd=200$ pF is 100nA at cryogenic temperatures and the transimpedance is 750 Ω . The specification limit (SR7) is reached for the preshaper output noise equal to 144 μ V, that is a safely above the preshaper noise.

The simulated non-linearity is less than 0.5% in the range up to 4V of the output signal.

Another important characteristic is a safeguard against oscillations. Since the preshaper consists of two stages the simulation has been done for both stages separately.

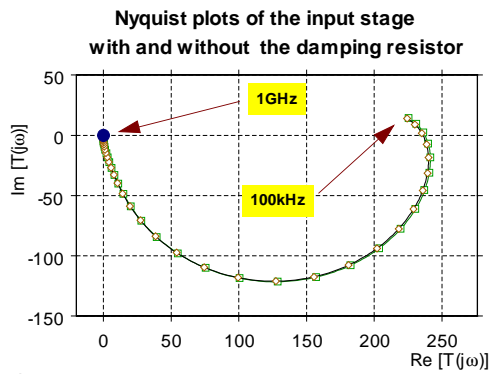
Stability of a linear system can be predicted by several methods. One of them is the analysis of Nyquist diagram. According to this method, the linear circuit is considered to be stable if the Nyquist plot for the function $T(j\omega)=1+B(j\omega) \cdot A_{oi}(j\omega)$ of the element should not encircle the critical point (0,0) in clockwise direction, where:

$A_{oi}(j\omega)$ - is the open loop gain of amplifier;

$B(j\omega)$ - the feedback return ratio.

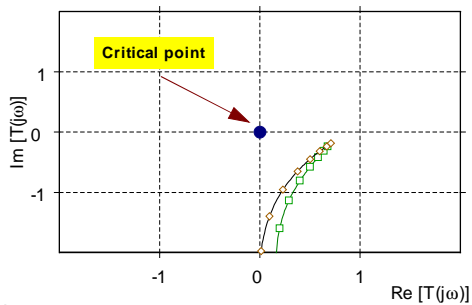
Diagrams (Figure 9) show that both stages are stable and the damping resistor adding in the Widlar triplet does not improve the stability of this scheme. And vice versa, the output serial resistor improves the stability when the output is loaded on the capacitance.

The second possibility to check stability is analysis of Bode plots. The linear amplifier is stable if the phase between output and input signals is less than 180° at unit-gain frequency. Bode plots for the first stage are shown on Figure 9.



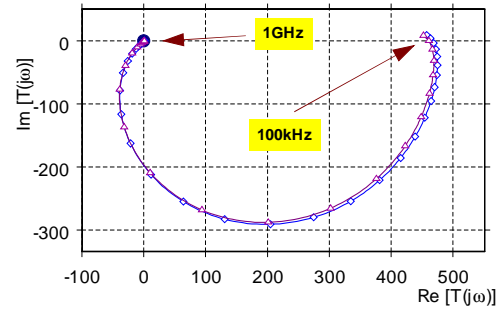
a) Full range plots

CI=50pF, β =nominal, $R_s=50\Omega$



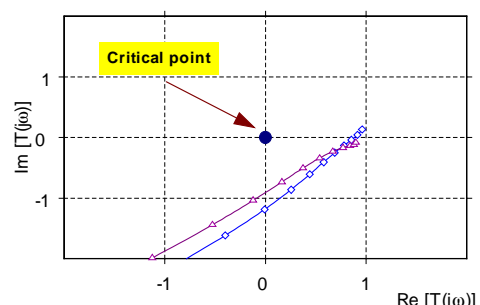
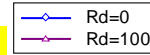
b) plots in the region of the critical point

Nyquist plots of the output stage with and without the damping resistor



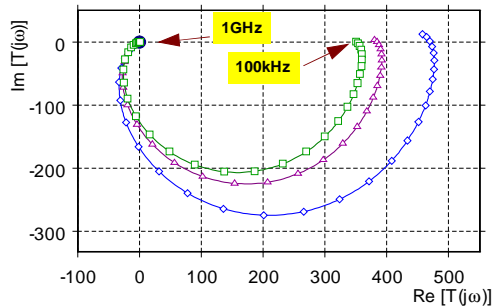
a) Full range plots

CI=50pF, β =nominal, $R_s=50\Omega$



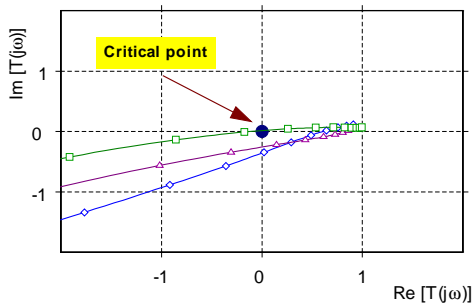
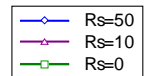
b) plots in the region of the critical point

Nyquist plots of the output stage with the different serial resistors



a) Full range plots

CI=50pF, β =nominal, $R_d=0$



b) plots in the region of the critical point

Bode plots vs the beta of transistors

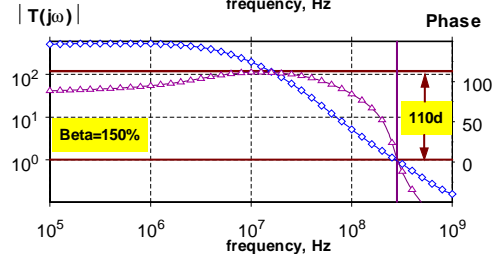
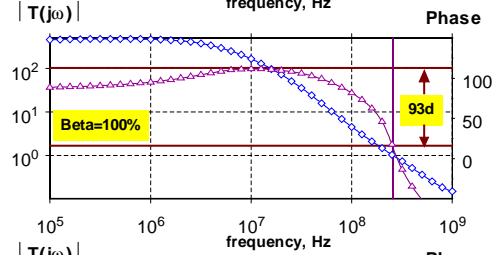
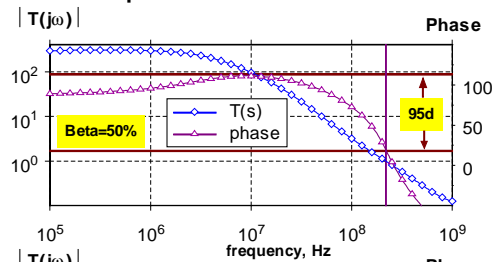


Figure 9: Simulation of preshaper stability by Nyquist diagrams and Bode plots (CI is loading capacitance, β - forward beta of transistors, R_d - damping resistor in Widlar triplet, R_s - output serial resistor).

Trigger level 1 requires the analog summation of signals after preshaper. Summation of channels with different amplification or peaking time violates the accuracy of trigger signal. Trigger system requires to have amplitude uniformity better than $\pm 5\%$. SPICE simulations show that peaking time variation up to $\pm 2.5\text{ns}$ distorts the amplitude of the summed signal up to $\pm 5\%$; and peak position shift up to $\pm 2.5\text{ns}$ distorts the summed amplitude only by $\pm 1\%$. So, the requirements to shape uniformity is much stronger.

Another important characteristic of preshaper is the power supply rejection ratio. Simulation shows that rejection of low frequency noise is:

- 40dB for supply of -3V
- 56dB for supply of $+3\text{V}$
- 54dB for supply of $+10\text{V}$.

These values are sufficiently high and can be accepted.

Required input impedance is provided by schematics and equals to about 50.5Ω in the working frequency range.

2.3 POWER CONSUMPTION

Table 2 shows currents and corresponding power, which hybrids consume from the supplies at nominal voltages. The values are given from SPICE. Calculated total power of a hybrid is 198.4mW that is within specification requirement **SR11**.

	Power (V)	Current 1ch (mA)	Current 1 hybrid (mA)	Power 1 hybrid mW	Current 1 FEB (mA)	Power 1 FEB Watt
Vdd	+10	3.9	15.6	156.0	499.2	4.99
Vcc	+3	0.63	2.52	7.6	80.64	0.242
Vss	-3	2.9	11.6	34.8	371.20	1.114

Table 2: Power consumption of preshaper.

Measurements in the laboratory conditions as well as on FEB-0 show that real consumption currents are very close to simulated. They are typically 2-3% less that can be explained by the fact that the real value of Vss was -2.9V instead of theoretical -3.0V .

3. Laboratory Tests

3.1 MEASURING SETUP

Measurements of the preshaper characteristics have been done when hybrids are plugged in the special test box. For signal measurements we used rectangular pulse generator HP831A and signals were digitized by oscilloscope TDS520. The instruments control and data read out have been done through GPIB bus with PC. The program is written in TESTPOINT software. Noise has been measured also by oscilloscope.

3.2 SIGNAL SHAPE ANALYSIS

The signal parameters – amplitude, integration time constant and zero time constant have been extracted by applying the fit of the measured waveforms by the model function. This function in the frequency domain is as follows:

$$U_{out}(s) = \frac{1}{s} \cdot \frac{U_g}{1+s \cdot \tau_g} \cdot \frac{1+s \cdot \tau_1}{1+s \cdot \tau_2} \cdot G_p \cdot \frac{1+s \cdot \tau_{pz}}{(1+s \cdot \tau_i) \cdot (1+s \cdot \tau_0)}$$

Where: U_g is the generator amplitude;
 τ_g is the pole of generator;
 τ_1, τ_2 are time constants of input cable;
 G_p is the preshaper gain;
 $\tau_{pz}, \tau_i, \tau_0$ are preshaper time constants.

Applying inverse Laplace transformation to this function, one can obtain an analytical expression in the time domain and use it to fit the measured waveform.

3.3 RISE TIME COMPENSATION

In the ideal case, the zero time constant τ_{pz} has to be equal to the preamplifier rise time τ_{pa} . The deviation of τ_{pz} from the predicted value gives a deviation of peaking time. The measured values of τ_{pz} as a function of predicted τ_{pa} are shown on Figure 10. Lines represent the region of τ_{pz} values where the peaking time deviates from required value of 50ns within ± 1 ns. Such a limit (instead of acceptable ± 2.5 ns) has been selected in order to have some safety margin for variation of other parts of HEC analog chain (cables, preamplifiers, etc.). The peaking time on the shaper output is computed as convolution of the measured preshaper signals and ideal RC^2 - CR shaper function.

The analysis has been done with τ_0 and τ_i fixed to 2ns and 14ns respectively. It is not necessary to take into account variation of τ_0 and τ_i , because a possible deviation of these parameters effectively contributes to the deviation of τ_{pz} .

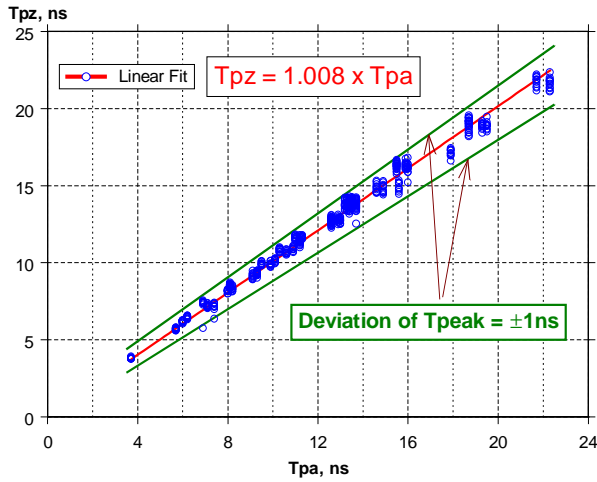


Figure 10: Measured zero time constant vs. predicted preamplifier time constant. Lines show the range where the peaking time deviation is ± 1 ns.

3.4 GAIN and GAIN UNIFORMITY

The gain of channels is extracted from signal responses. Figure 11 shows the distribution of gains for all tested channels. The ratio between high and low gains of preshaper is equal to 2.04, that is in the required range.

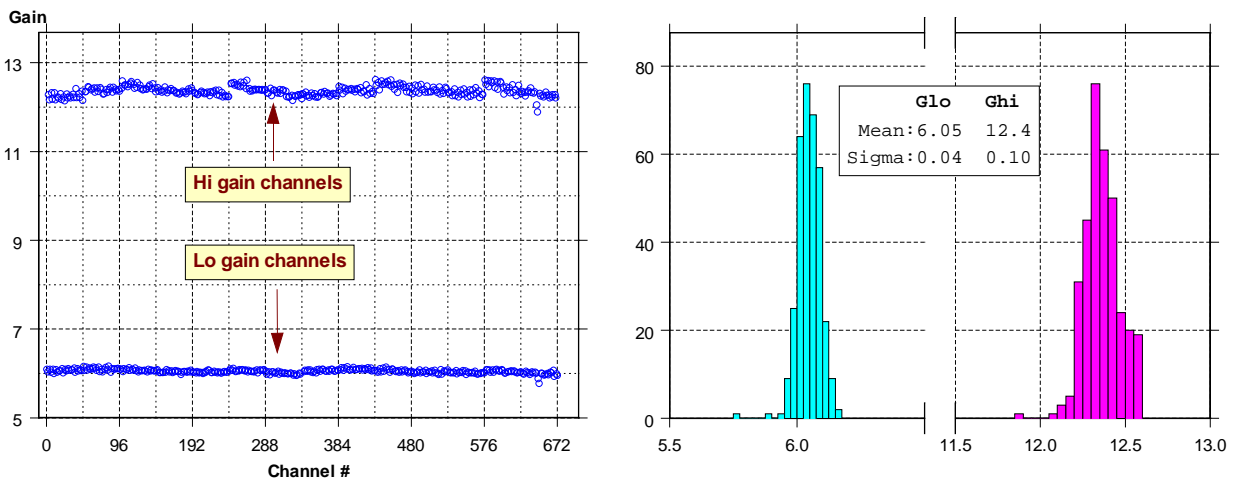


Figure 11: Gain gain distribution of preshaper channels (168 hybrids).

The gain uniformity (Figure 12) is estimated as deviation of each gain from the value averaged over all tested hybrids. In order to have the same scale for all channels, the high gains are divided by factor 2.0. The full dispersion of gain is 5% and the RMS is less than 1.5%. These values are close to the expected ones, because the mounted resistors have tolerance of 1% and the capacitors have tolerance of 5%.

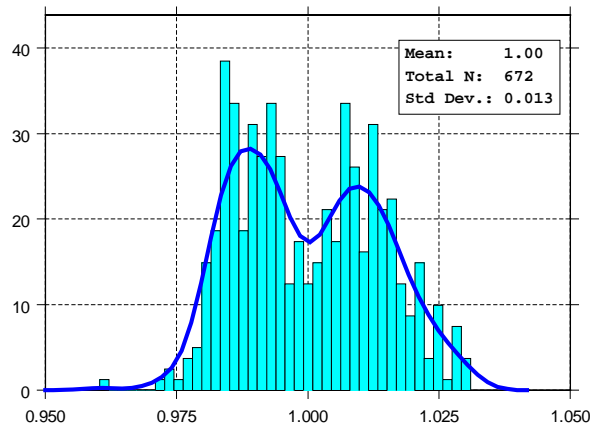


Figure 12: Gain uniformity (the left peak is Lo gain channels and right is Hi gain channels).

3.5 NOISE PERFORMANCE

Noise has been measured on the preshaper output by digital oscilloscope in full frequency range (500MHz). Figure 13 shows the distribution of the noise RMS values for low gain and high gain channels as function of the corresponding detector capacitance. The values expected from SPICE model are given as lines. These numbers are in good agreement with measured values.

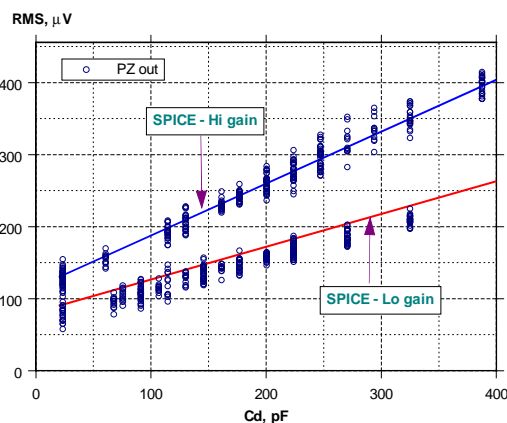


Figure 13: Noise RMS voltage on the preshaper output vs. detector capacitance. Lines are the SPICE simulation.

The predicted Equivalent Noise Current (ENI) of cold preamplifiers and contribution of preshaper to the ENI for all 51 different readout channels of HEC module are shown on Figure 14. The acceptable QC-level (SR7) is also presented here.

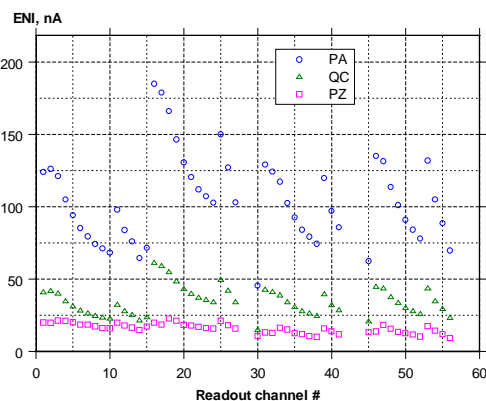


Figure 14: Predicted equivalent noise current of preamplifiers (PA), preshaper quality control level (QC) and measured values (PZ).

3.6 PRESAPER PERFORMANCE ON FEB0

The reason of the tests was to make the performance measurements of HEC preshaper on the FEB0. Usual characteristics as noise, transfer function and Xtalk have been studied. The measurements have been carried out at Brookhaven National Laboratory (BNL). The BNL test setup (Figure 15) consisted of the standard front-end crate, read out system (TTC, SPAC, ROD), precision delay unit and rectangular pulse generator. The delay unit was programmed by computer and allowed to measure the signal waveforms with step of 1ns. The software has been written by Francesco Lanni and Kin Yip.

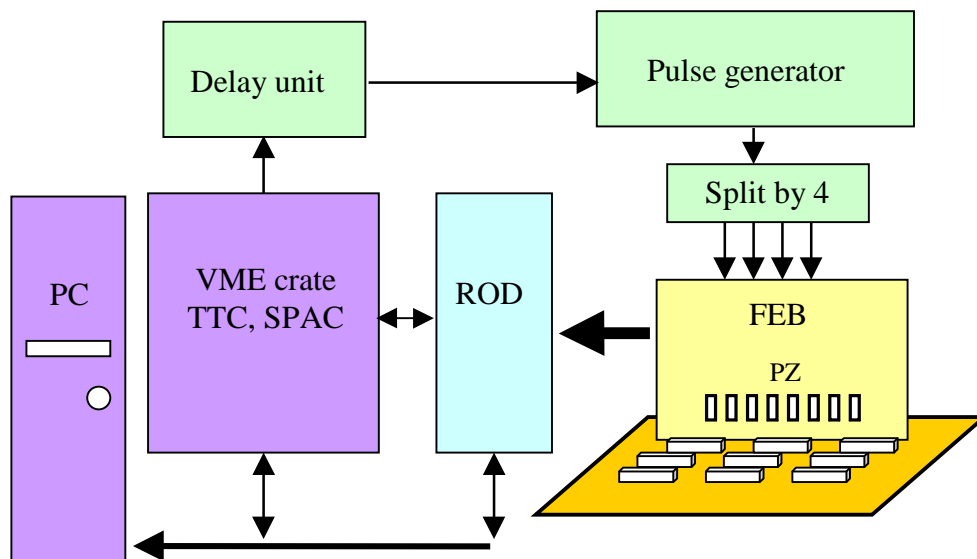


Figure 15: BNL test setup.

The hybrids have been plugged in the place of OT preamplifiers on the FEB. The mechanical compatibility is perfect. The power checking showed, that the standard FEB0 cannot be equipped with all 32 pieces of hybrids simultaneously, because the negative supply drops down to -2.5V, and that is out of working range for preshaper. Therefore all tests carried out with simultaneous installation of 16 hybrids and, in this case, the voltage was -2.75V.

Explanation has been found later by studying of FEB0 at MPI. The negative voltage $V_{ss} = -3V$ for preshapers is produced by the regulator LM2991 equipped by external serial resistor of 3Ω at the output. The observed shift of the V_{ss} was due to the voltage drop on this resistor

Noise performance

RMS of noise has been measured and afterwards recalculated to the preamplifier input. The contribution of preshaper to the ENI is less than 20nA (Figure 16). The measured noise has been compared with SPICE simulation. The real noise is in a good agreement with simulated, but usually higher at 10% (Figure 17).

The noise auto correlation function has been measured in two points: at the readout output and at the output of the layer summing board (LSB). The coherent noise seen by ADC is typically about 2%, but at the LSB output it is much higher (Figure 18). Here the dominant frequencies are 5MHz and few hundreds MHz. The first is the clock of ADC, and second one is probably an oscillation of LSB, because only one output was loaded.

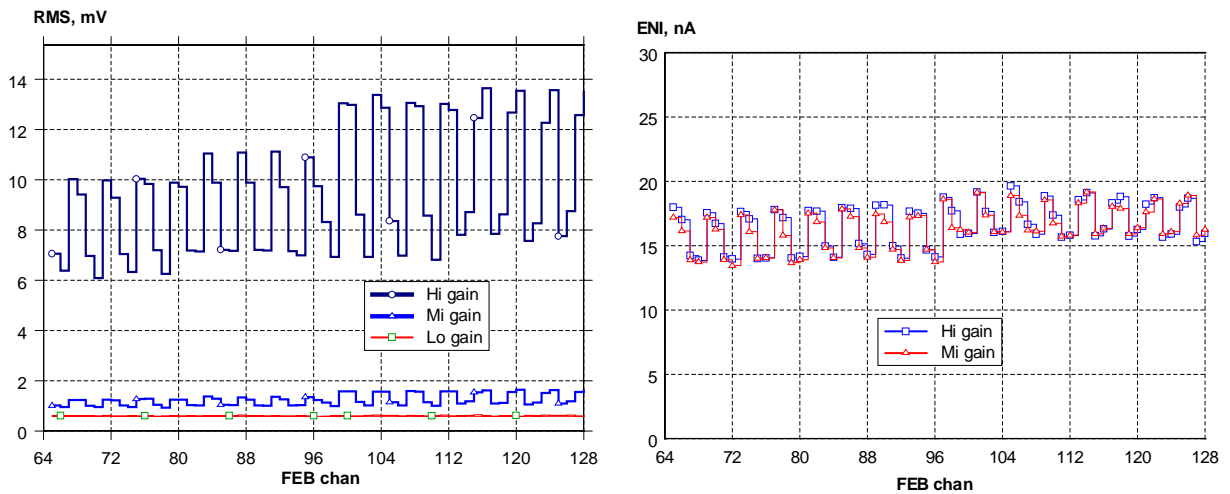


Figure 16: FEB0 output RMS noise (left) and equivalent noise current (right) for different gains of shaper .

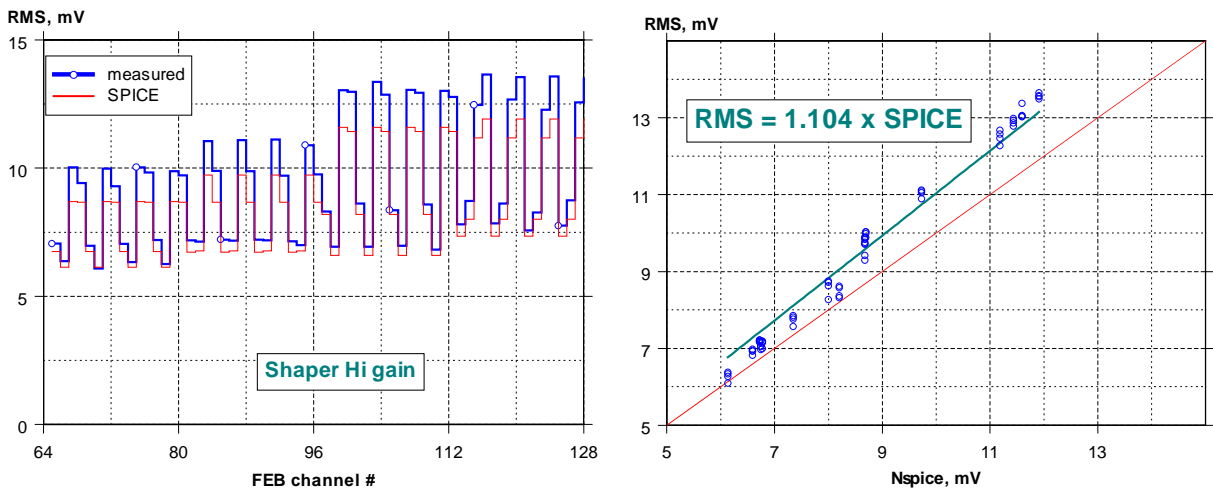


Figure 17: Comparison of measured and simulated noise values.

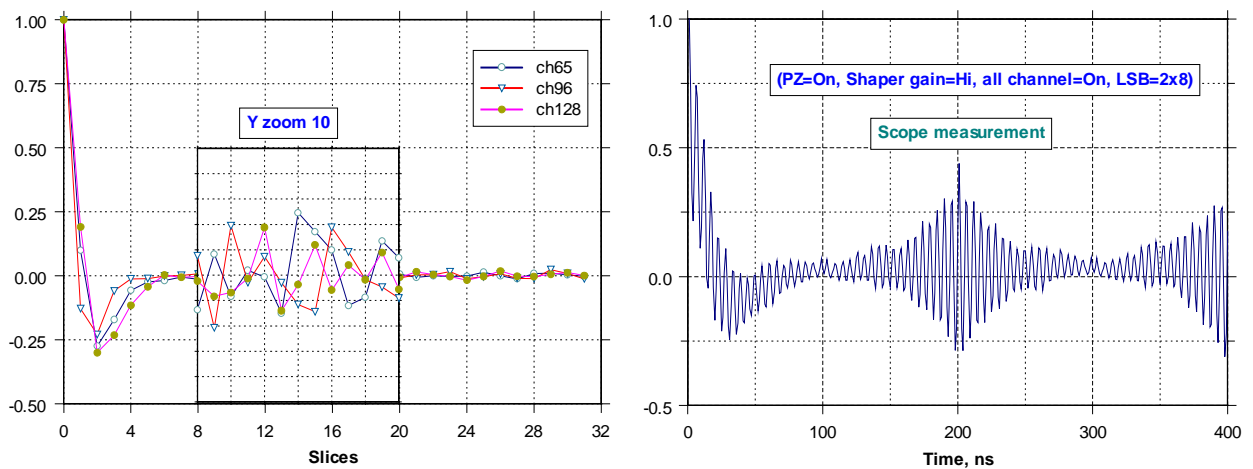


Figure 18: Noise auto correlation function at the readout output (left) and LSB output (right).

Transfer function

Transfer function has been measured with three gains of the shaper. The measured parameters have been compared with SPICE simulation. It has been found that FEB0 has an additional pole of 5ns. The mean value of shaper time constant has been determined as 13.7ns for high and middle gains, and 14.5ns for low gain. An example of step responses of four channels is shown on Figure 19.

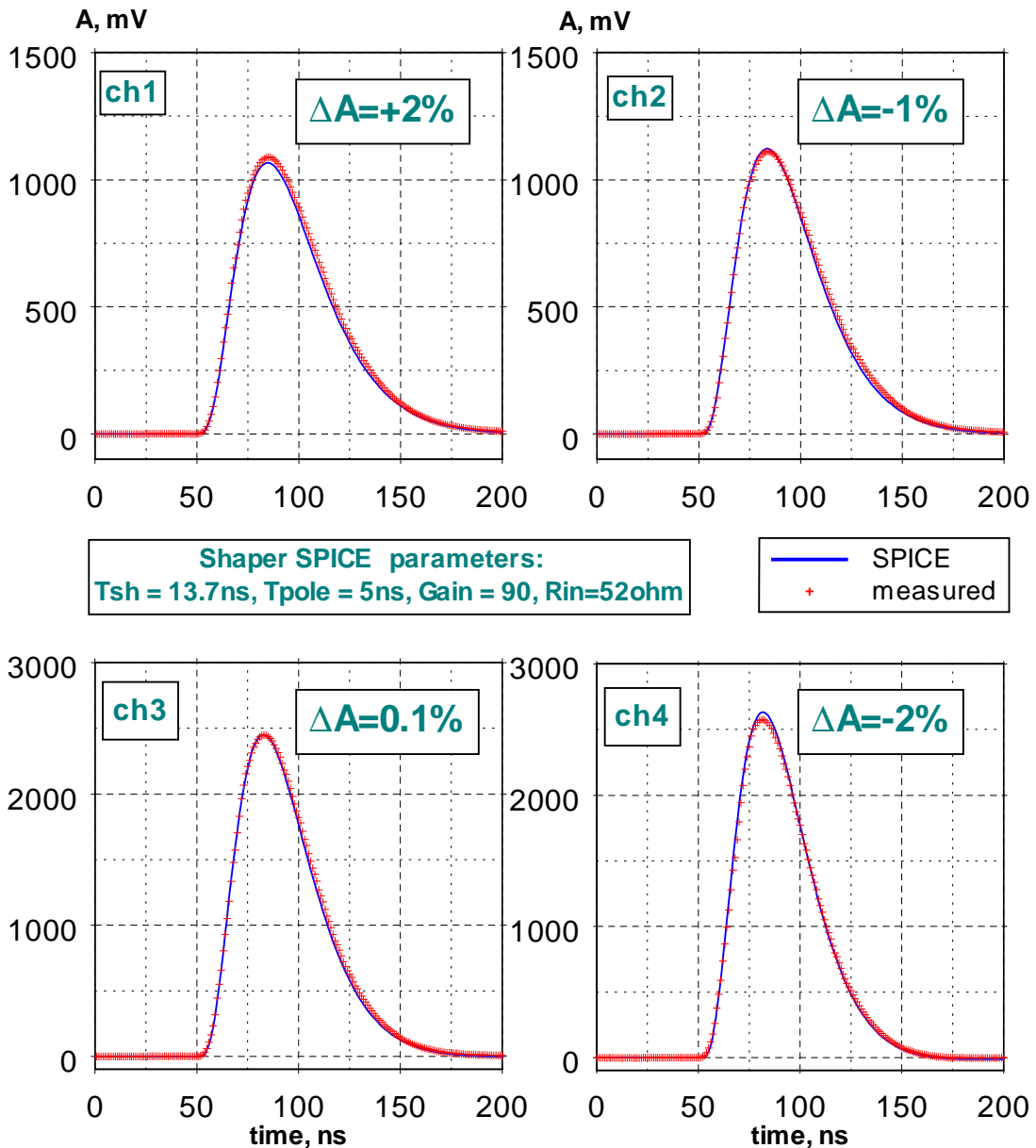


Figure 19: Measured and simulated step responses of the FEB0 with HEC preshaper.

Rise time compensation

The values of τ_{pz} are within the QC window (Figure 20). The reconstruction has been done without taking into account a possible spread of the shaper time constant, which is about $\pm 0.5\text{ns}$.

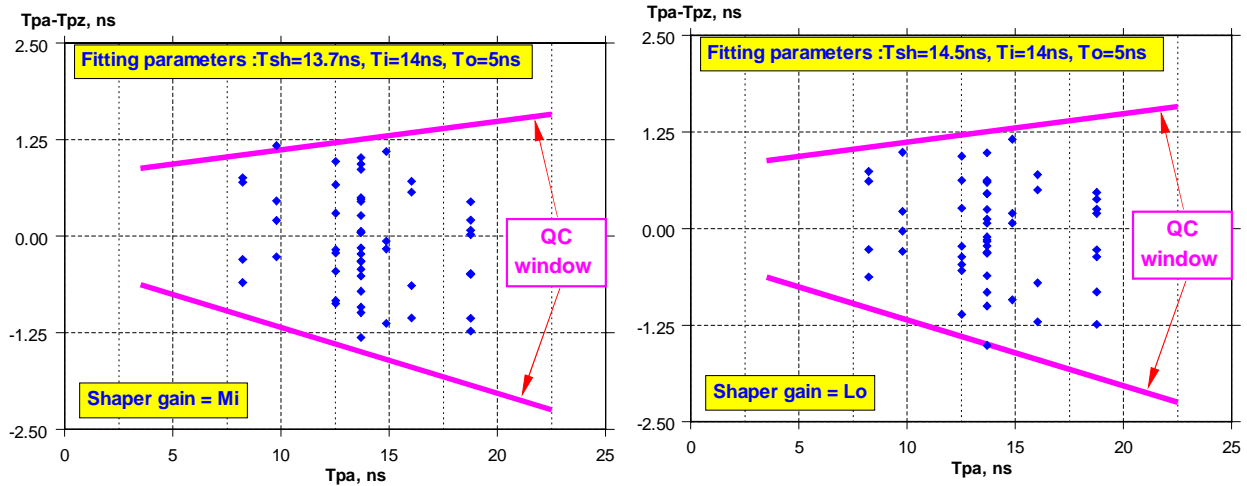


Figure 20: Preshaper rise time compensation constant for two gains of shaper.

Gain

Preshaper has two different gains for front and rear modules. Figure 21 shows distribution of the FEB channels for the middle gain shaper output. The ratio between high and low gain channels has to be equal to 2.0. Measured ratio is 2.036.

Xtalk

The Xtalk between neighboring chips has been found as 0.5% (Figure 22).

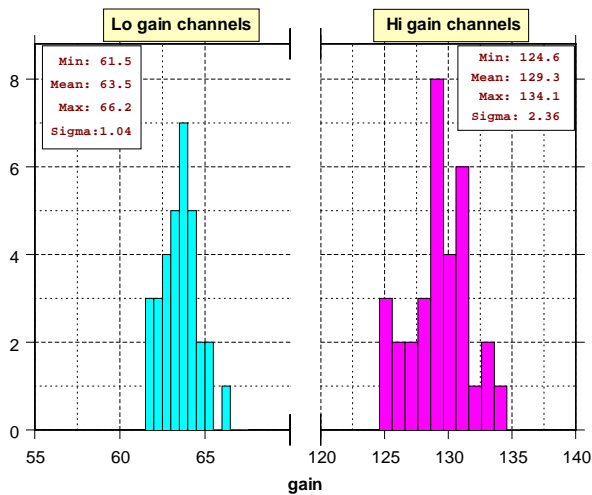


Figure 21: Distribution of FEB channel gains (shaper gain is middle).

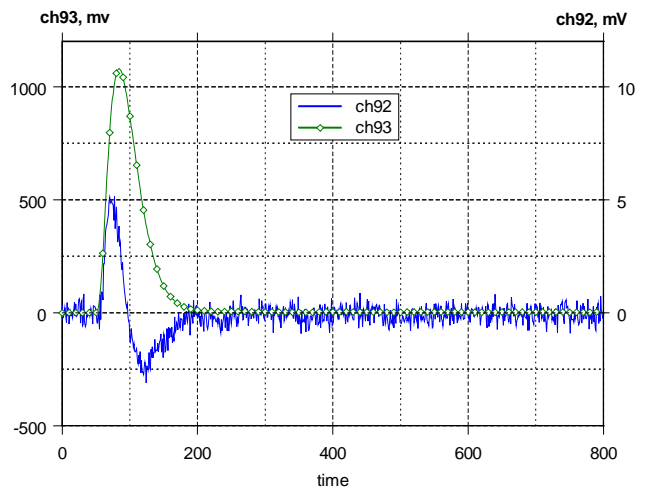


Figure 22: Xtalk between two channels of the neighboring chips.

4. Test Beam Results

4.1 TEST BEAM ELECTRONICS

During 2001 two beam periods took place - in July and in August. The setup in both periods was identical. 32 preshaper hybrids (128 channels) have been installed in one FEB version -1 that allowed reading the beam area channels. This setup was used for the standard calibration procedure and few physical runs have been taken.

4.2 PRESHAPER CHARACTERISTICS

Using the standard calibration procedure, the noise, gain, gain uniformity and peaking time values have been measured and compared with predictions.

Figure 23 shows the response to the calibration signal and waveform predicted by SPICE. A difference between measured and simulated waveforms can be explained by Xtalk in HEC readout electrodes.

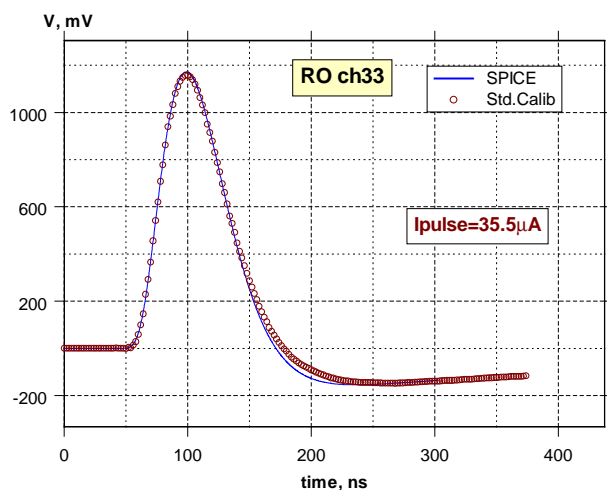


Figure 23: *The typical calibration signal, measured for one of the HEC channels and prediction obtained with nominal parameters of the chain.*

The peaking time of calibration signals have the mean value of 51.2ns and RMS of 1.3ns. That is in a good agreement with simulation (52.1ns). Distribution of the peaking time is shown in Figure 24.

The amplification of channels is shown in Figure 25. Absolute numbers are close to the expected values. The RMS of gains is 8%. The ratio between high and low gains is 2.06.

The rise time compensation by the preshaper can be seen in the correlation between the peaking time and detector capacitance. In the absence of compensation, some strong correlation should be observed. If the compensation is ideal, no correlation will be seen. Figure 26 shows this correlation plot. Within the spread of points, the correlation is very small. The same effect can be studied by looking at the correlation between gain and detector capacitance. As in the previous case, the wide spread of amplitudes shows no correlation.

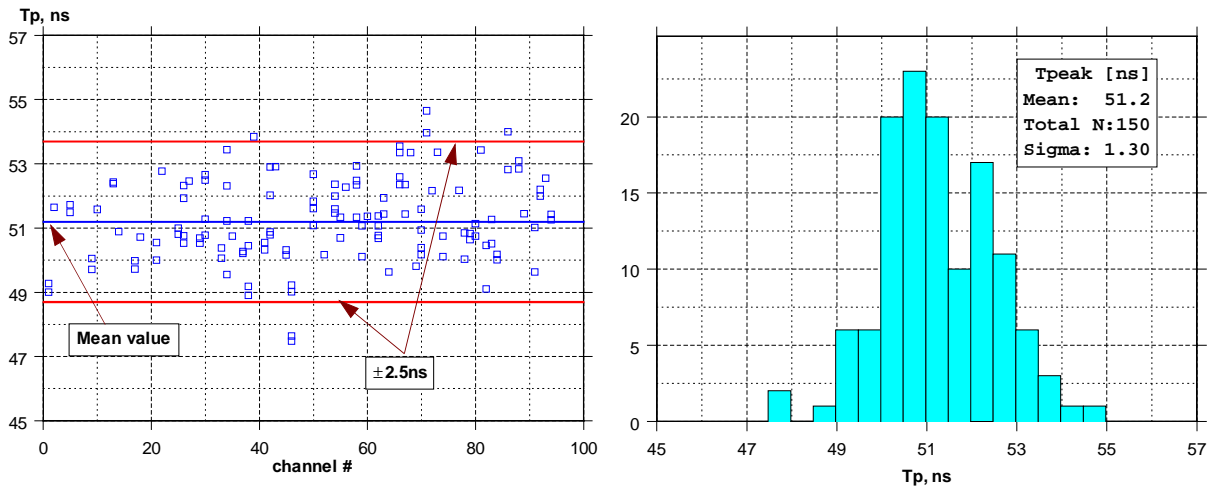


Figure 24: Peaking time distribution from the calibration procedure.

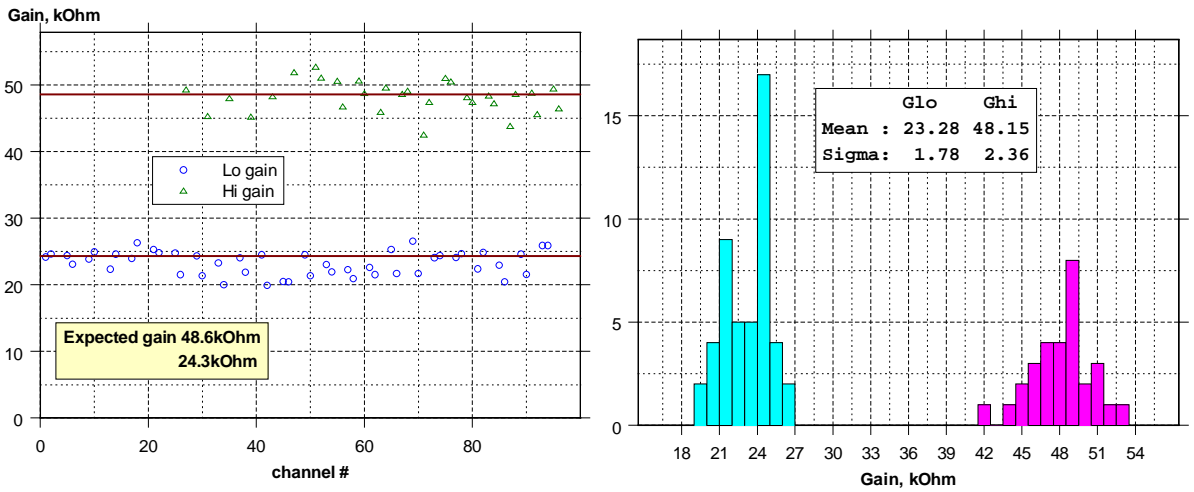


Figure 25: Amplification measured with calibration signals.

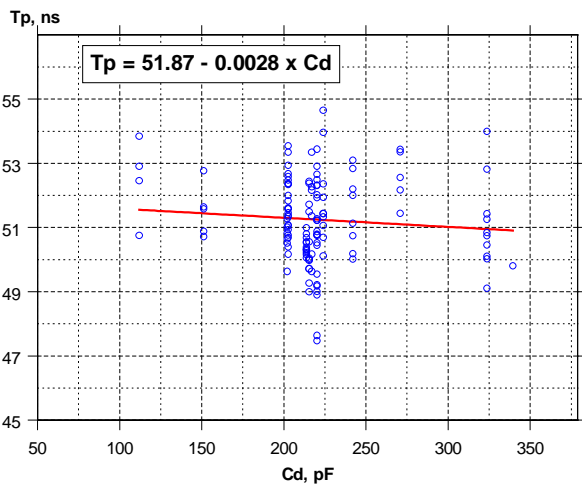


Figure 26: Correlation between peaking time and detector capacitance.

4.3 NOISE OF HEC CHAIN

It was found that most of the read-out channels in the test-beam conditions have noise values equal to expected. At the same time there are noisy channels, all of them are located in one edge of each FEB. This is demonstrated in Figure 27. The study of the noise autocorrelation functions shows that this noise have oscillating nature. It was also observed that there is strong correlation between neighbouring noisy channels, so this oscillation is coherent. Figure 28 shows autocorrelation functions of the first four channels on FEB measured by oscilloscope and by FADC. This effect is known and has been studied and identified. The main contribution to coherent noise is the pick-up noise from FADC, which goes directly to FEB. The disconnection of FADC cables decreasing this noise significantly.

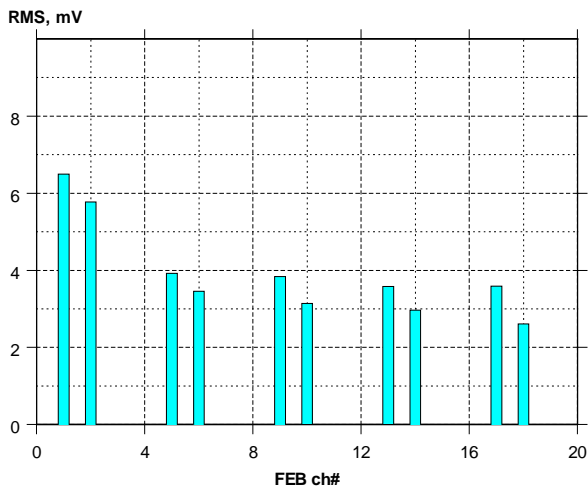


Figure 27: Noise RMS value for the first 20 channels (3 modules) of the FEB version -1.

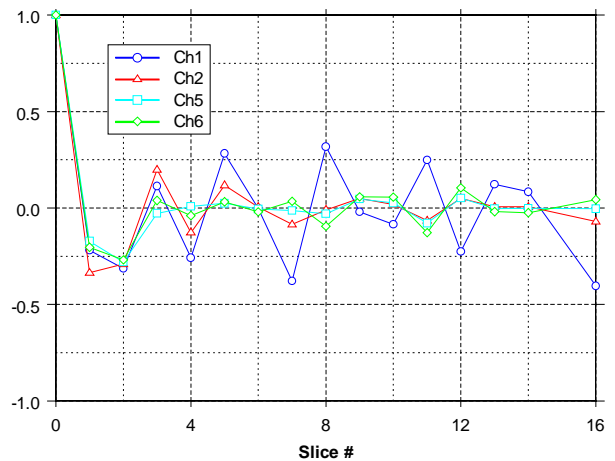
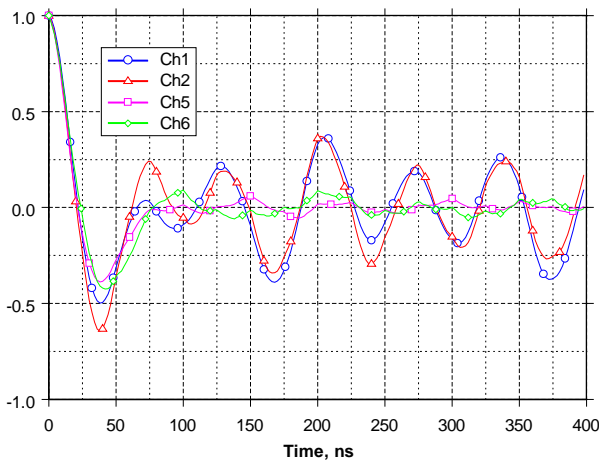


Figure 28: Noise autocorrelation function of four noisy channels (left: measurement by scope, right: by FADC).

4.4 PHYSICAL WAVEFORM

Few physical runs in four different points of modules have been taken. The signals have been fitted by standard function and peaking time values were found. They are in the range between 48.1ns and 48.3ns. Figure 29 shows the signal of 119GeV electron in the point 'K' (ADC29) and expected waveform calculated from the calibration.

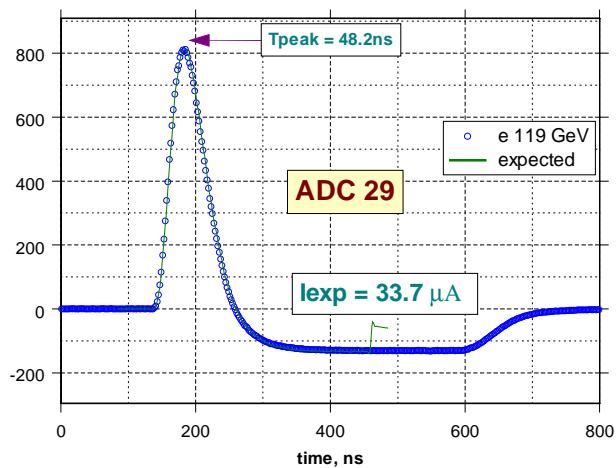


Figure 29: Signal from electrons of 119GeV and expected signal predicted from calibration.

5. Radiation Tests

Since the preshapers will be placed inside the End-Cap Front-End Crate, it is necessary to test them for radiation hardness according to LAr Radiation Tolerance Criteria figures (Table 3).

	Simulated dose	SF sim	SF ldr	SF lot	RTC
γ , Gy	5	3.5	5	4	350
n/cm^2	$1.6 \cdot 10^{11}$	5	1	4	$3.2 \cdot 10^{12}$

Table 3: Radiation tolerance criteria SF – safety factors.

The neutron irradiation of 10 hybrids version 0 has been carried out in December 1999 at IBR-2 reactor in Dubna [10]. The total fluence was achieved up to $2.7 \cdot 10^{14}$ of neutron per cm^2 and accumulated γ -dose of 1200Gy. Accuracy of the doses measurement is $\pm 10\%$.

The measuring setup for the testing of the cold GaAs preamplifiers was used [11]. Preshaper characteristics have been measured after RC²-CR shaper with different time constants. The typical dependence of the signal amplitude vs. the neutron dose is shown in Figure 30. It was measured for 4 different shaper time constants, for 25ns-shaping time (most close to working conditions) the effect is less than 1% in the required dose range. For all shaping times, the amplitude drop of all tested channels varies in the range of 3%. The same plot for the peaking time is shown in Figure 31. No significant changes can be seen. The relative changes of the peaking time do not exceed 2% for 40 channels.

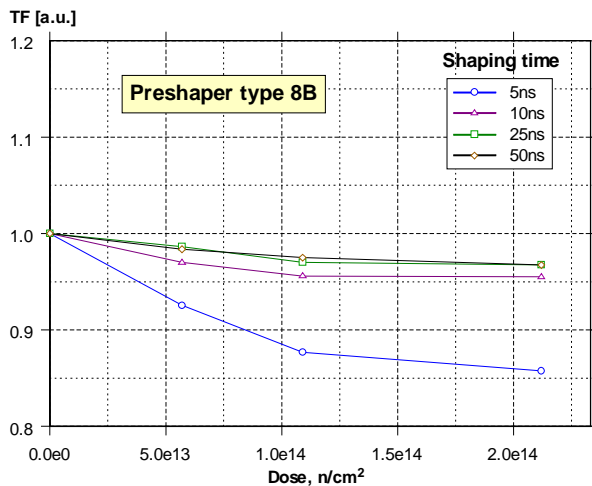


Figure 30: Relative amplitude degradation vs. the neutron fluence.

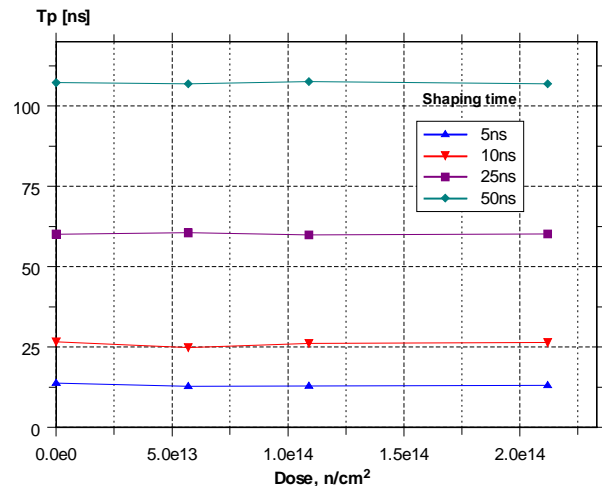


Figure 31: Peaking time after RC²-CR shaper vs. the neutron fluence.

Measurements of the linear range are demonstrated in Figure 32. For all neutron doses the dynamic range is under the specification value of 4V. No change in linearity was observed for all channels.

Noise has been measured on the shaper output and then recalculated to the preshaper input. It is shown in Figure 33 as a function of the fluence. No changes can be seen within measurement errors (~20%).

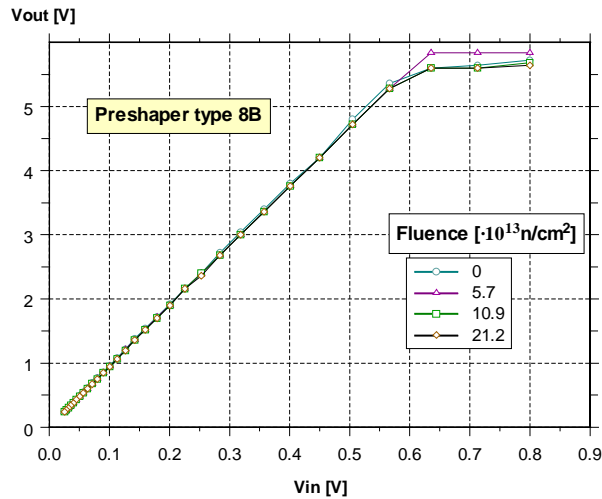


Figure 32: Behaviour of the linear range vs. neutron fluence.

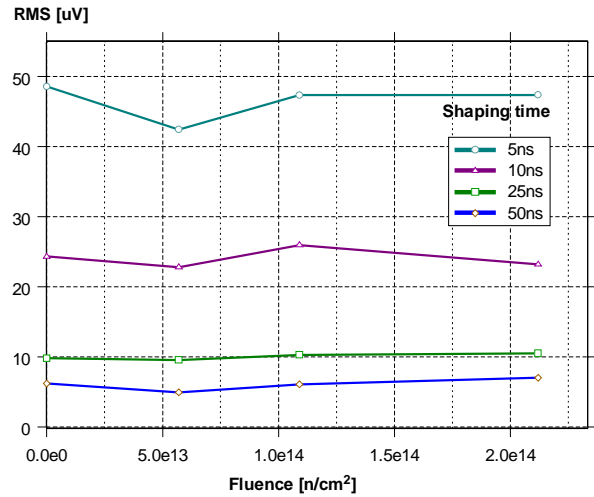


Figure 33: Behaviour of the related to input preshaper noise vs. neutron fluence.

Summarising the radiation tests results, we can say that for the neutron fluence up to $2.7 \cdot 10^{14}$ n/cm² including γ -dose of 1200Gy no channel of 40 is dead. No big changes of parameters were seen.

Version 1 of preshaper was not irradiated, but its design is very similar to the previous version and no new components are used. It can be expected that the radiation hardness should be the same. Nevertheless our plan is to make the radiation tests with hybrids from the first production batch in the fall of 2002.

6. Burn-in Test and Failure Rate

The batch of hybrids produced (168 units) after being tested for electrical functionality was subjected to 168 hours of a burn-in at the 100°C temperature to identify early failures. In order to detect any possible variation of parameters all hybrids were characterized in term of gain, time constant and noise before and after the burn-in.

During the tests only one channel failed, because the soldered contact of a decoupling capacitor was lost. After repairing the channel works perfectly.

Figure 34 shows the comparison of the noise, gain and zero time constant before and after the burn-in.

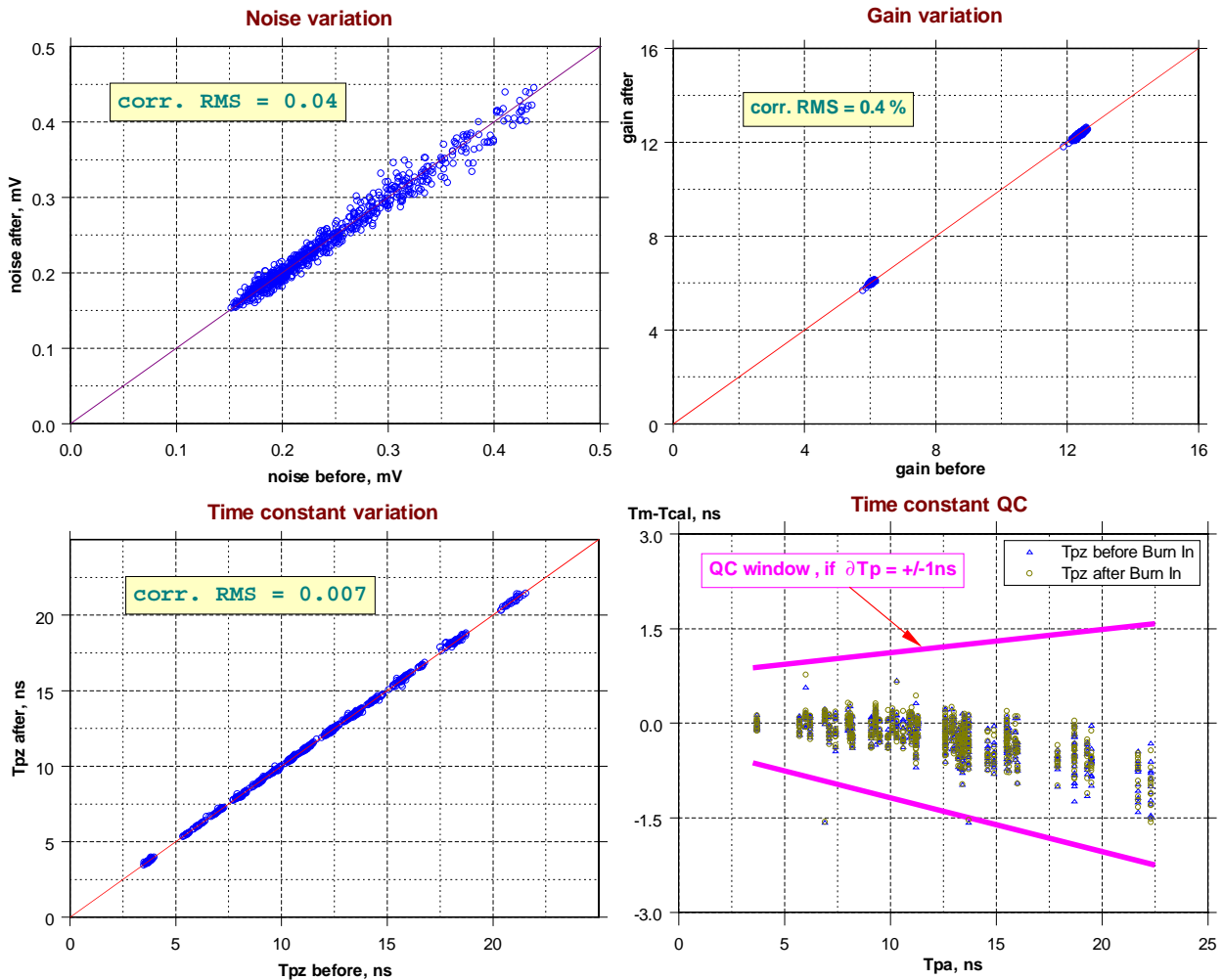


Figure 34: Preshaper parameters measured before and after the burn-in.

All channels did not change their characteristics during the burn-in test. Only some fluctuation within the range of measuring errors can be seen. So the RMS of noise variation is 4%, RMS of gain variation is 0.4% and RMS of time constant variation is 0.7%. Time constant of two channels is out of the QC range and that was before the burn-in.

Since we did not find a variation of parameters it was decided to make in future the high temperature treatment only before the functionality tests. It can be done by the producer.

7. Quality Control of the Preshapers

We propose the quality assurance procedure consisting of few steps:

1. **The high temperature treatment procedure as the last step of production.**
Each hybrid must be kept 100 hours at 100°C
2. **Visual inspection.** In particular, the accordance of the specified components to the type of hybrids has to be checked.
3. **DC-tests.** The potential has to be measured in specified points in order to check the working conditions of transistors, shortages and missing connections.
4. **Functionality tests.**
All important characteristics have to be measured and compared to a window of acceptable values:
 - Step response measurement and analysis for the time constant and amplification factor
 - Linearity
 - Crosstalk (few pieces from each batch)
 - Noise
5. **Hybrids, which do not pass the tests, will be rejected.**

The setup for the functionality tests is schematically shown in Figure 35. Rectangular pulse generator produces input pulse, which goes to four channels through splitter. Output signals are digitized by oscilloscope and read out by PC through GPIB bus. The control program is realized using TESTPOINT software. The program allows to measure all four channels of hybrid simultaneously. The special fitting program reconstructs the parameters (G_p and τ_p) from the output signal.

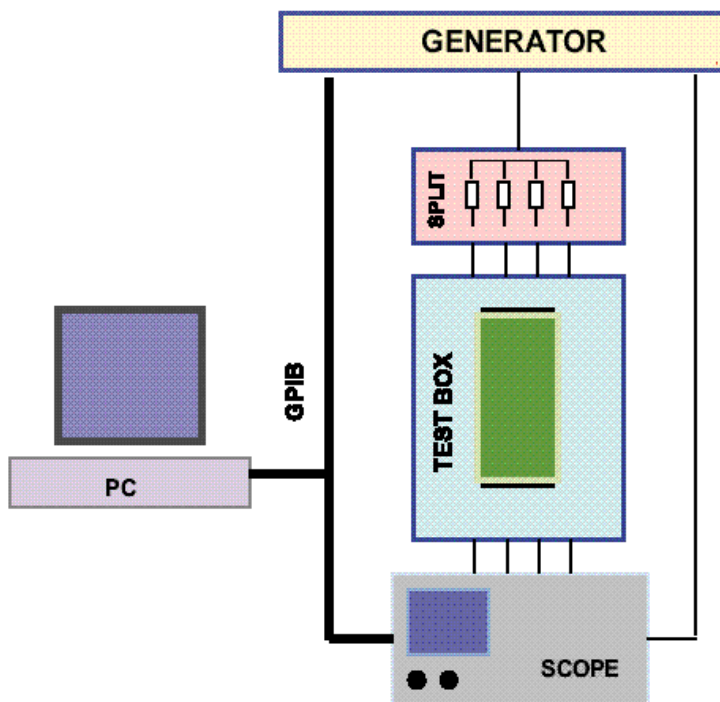


Figure 35: Setup for the functionality tests.

168 pieces of version 1 produced in April of 2001 have been measured following this QC procedure.

- 10 hybrids have mistakes of the mounting (usually soldering short), one has the internal shorted line.
- Zero time constant of two channels is out the QC window (Figure 34).
- Non-linearity of all channels is within QC window.
- Gain uniformity of 16 channels is out of $\pm 2.5\%$ (Figure 12).
- The measured equivalent noise current (ENI) is in the required range.

8. Production Plans

The production plan presented here is in agreement with the present ATLAS master plan and is based on the ATLAS and LAr detector milestones. The full amount of hybrids needed for HEC is the following:

- **For ATLAS:** **1536 hybrids**
- **Spare:** **288 hybrids**
- **Production:** **1824 hybrids**

The aim of the project is to have full amount of hybrids by the end of 2003. The most important dates for next years and actions foreseen for these two years are shown in Table 4.

Date	Action	Responsibility.
09.2002	Produce 960 hybrids	E.L.
09-12.2002	Lab tests	E.L. & L.K.
09-11.2002	Equip FEBs for FEC system test	??
11-12.2002	Rad. tests	E.L.
01-07.2003	Produce 864 hybrids	E.L.
08-12.2003	Lab tests	E.L. & L.K.

Table 4: *Preshaper production and tests in 2002-2003.*

So, the production schedule is:

- 2002: production of first 960 hybrids
- 2003: production of additional 864 hybrids

References

- [1] CERN/LHCC/96-41 (1996) ATLAS Liquid Argon Calorimeter TDR, ch. 10
- [2] ATLAS HEC Note-028 (1997) ATLAS Liquid Argon Calorimeter Collaboration Meeting on HEC Electronics. Munich, February 19 - 21, 1997
- [3] ATLAS HEC Note-073 (1998) Timing adjustment of HEC signals
- [4] ATLAS HEC Note-094 (2000) Preshaper for the Hadron End-Cap Calorimeter, Design Review
- [5] ATLAS HEC Note-066 (1998) HEC cold cables. Signal shape analysis
- [6] ATLAS Level-1 Trigger TDR, ch. 6.2.1.6
- [7] J. Collot, D. Dzahini, C. de La Taille, et al., *The LAr Tri-Gain Shaper*, ATLAS Internal Note LARG-No-92 (1998)
- [8] ATLAS Radiation Hard Electronics Web Page: see <http://atlas.web.cern.ch/Atlas/GROUPS/FRONTEND/radhard.htm>
- [9] ATC-TE-QA-001, ATLAS Policy on Radiation Tolerant
- [10] A.Cheplakov et al., Joint Institute for Nuclear Research, Dubna, preprint E13-96-358, 1996.
- [11] A.Cheplakov et al., Large-scale samples irradiation facility at the IBR-2 reactor in Dubna, NIM, A 411 (1998), p.330-336.

Appendix A: HEC electronic chain

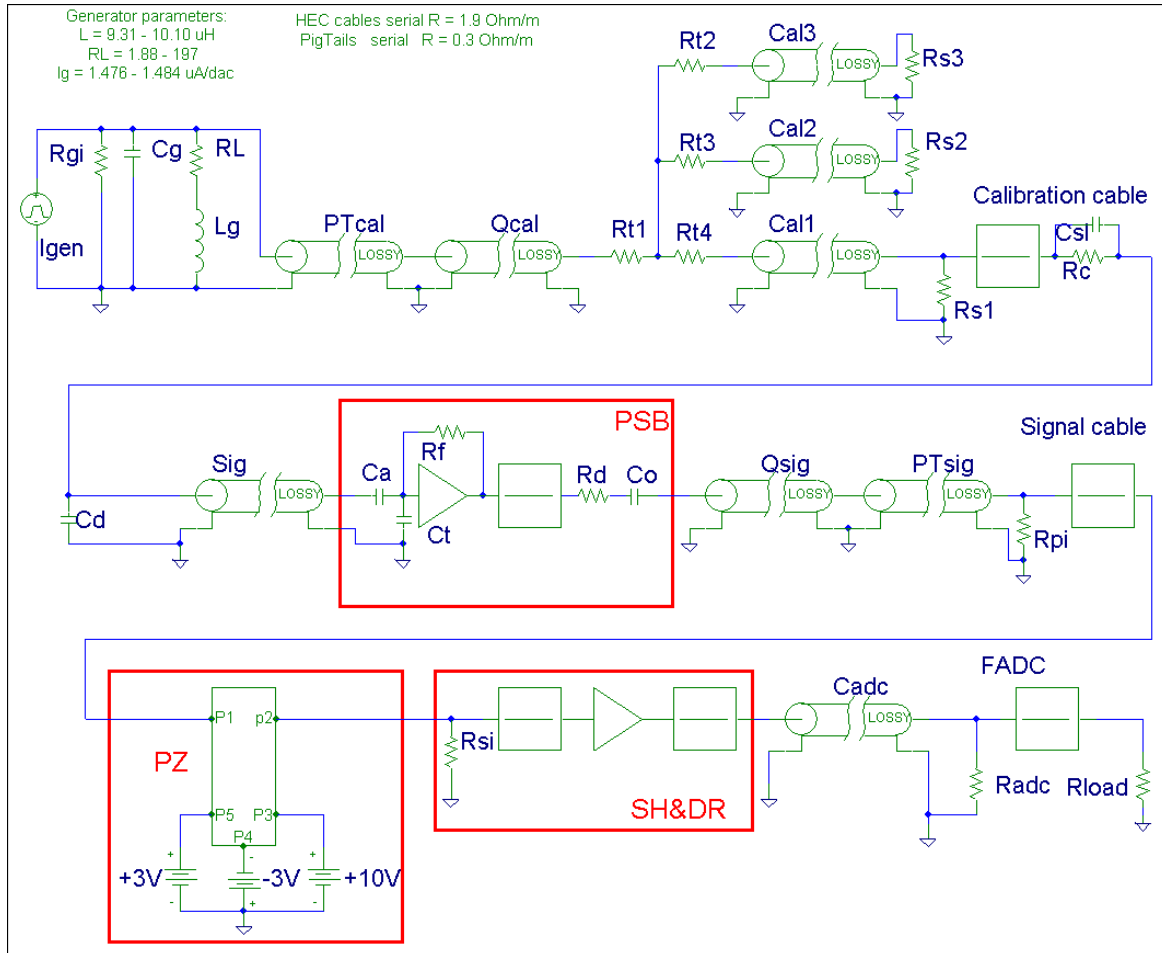


Figure A1: Test-beam HEC electronic chain model.

Generator voltage	$I_g \cdot R_l \cdot \frac{\alpha + s \cdot \tau_c}{s \cdot (1 + s \cdot \tau_c)} \cdot \frac{1}{3} \cdot \frac{1}{R_c + R_{in}}$	
	where	$R_l = \frac{R_{ig} \cdot (R_t + R_{cc})}{R_{ig} + R_t + R_{cc}}, \quad \alpha = \frac{R_g}{R_l + R_g}, \quad \tau_c = \frac{L_g}{R_l + R_g}$
Calibration cable	$\frac{ac \cdot (1 + s \cdot \tau_{zc})}{(1 + s \cdot \tau_{oc})(1 + s \cdot \tau_{pc})}$	where $ac = \frac{R_t}{R_t + R_{cc}}$
PSB	$\frac{R_p}{(1 + s \cdot \tau_a) \cdot (1 + s \cdot \tau_d)}$	where $\tau_a = R_a \cdot (C_d + C_a)$
Signal cable	$\frac{as \cdot (1 + s \cdot \tau_{zs})}{(1 + s \cdot \tau_{os})(1 + s \cdot \tau_{ps})}$	
Preshaper	$\frac{G_p \cdot (1 + s \cdot \tau_{pz})}{(1 + s \cdot \tau_i)(1 + s \cdot \tau_o)}$	
Shaper, FEB driver, ADC cable	$\frac{G_s \cdot s \cdot \tau_s}{(1 + s \cdot \tau_s)^3 (1 + s \cdot \tau_{fd}) \cdot (1 + s \cdot \tau_{ac})}$	
Calibration signal on pad level	$\frac{I_g \cdot R_l \cdot ac}{3 \cdot (R_c + R_{in})} \cdot \frac{(\alpha + s \cdot \tau_c)(1 + s \cdot \tau_{zc})}{s(1 + s \cdot \tau_c)(1 + s \cdot \tau_{oc})(1 + s \cdot \tau_{pc})}$	
Signal chain transfer function	$\frac{R_p a_s G_p G_s \tau_s \cdot s \cdot (1 + s \cdot \tau_{zs})(1 + s \cdot \tau_{pz})}{(1 + s \cdot \tau_i) \cdot (1 + s \cdot \tau_l)(1 + s \cdot \tau_o s)(1 + s \cdot \tau_{ps})(1 + s \cdot \tau_i)(1 + s \cdot \tau_o)(1 + s \cdot \tau_s)^3 (1 + s \cdot \tau_{fd}) \cdot (1 + s \cdot \tau_{ac})}$	

Table A1: HEC chain model functions.

Part	Parameter	Warm	Cold
Generator	$I_g, \mu\text{A}/\text{dac}$	1.48	---
	R_{ig}, Ω	50	---
	R_g, Ω	1.97	---
	$L_g, \mu\text{H}$	10.0	---
Calibration current	Splitting	1/3	1/3
	R_t, Ω	50	50
	R_c, Ω	5620	5620
Calibration cable	R_{cc}, Ω	14.1	5.4
	τ_{zc}, ns	12.2	18
	τ_{oc}, ns	1.9	1.2
	τ_{pc}, ns	18.5	21.8
Detector	C_d, pF	16 – 270	24 - 410
PSB	$R_p, \text{K}\Omega$	0.70	0.75
	R_a, Ω	70	50
	C_a, pF	40	50
	τ_d, ns	7	4
Signal cable	as	0.884	0.965
	τ_{zs}, ns	13.3	24.5
	τ_{os}, ns	1.63	1.18
	τ_{ps}, ns	17.2	28.5
Preshaper Version 1	G_p	6.15 (12.3)	---
	τ_{pz}, ns	$(C_d+50\text{pF})\cdot 50\Omega$	---
	τ_i, ns	14	---
	τ_o, ns	2.0	---
Shaper	G_s	8.3	---
	τ_s, ns	13.7	---
FADC	τ_{fd}, ns	2	---
	τ_{ac}, ns	3	---

Table A2: Parameters of the HEC chain.

Appendix B: Component list of preshaper

#	Q-ty	Package	Reference	Value/type
1	20	Pin	X2 X19 X20 X10 X9 X3 X4 X17 X18 X5 X6 X15 X16 X7 X8 X13 X14 X11 X1 X12	(*)
2	16	Sot323	Q8 Q11 Q13 Q15 Q16 Q19 Q21 Q23 Q24 Q27 Q29 Q31 Q32 Q3 Q5 Q7	BFR92w
3	16	Sot323	Q9 Q10 Q12 Q17 Q18 Q20 Q25 Q26 Q28 Q1 Q2 Q4 Q36 Q35 Q34 Q33	BFT92w
4	4	Sot23	Q30 Q6 Q14 Q22	BFR194
5	4	Cc1206	C4 C6 C8 C2	1.0 μ F/16V
6	16	Cc0805	C14 C17 C18 C20 C23 C24 C26 C29 C30 C32 C12 C11 C36 C35 C34 C33	0.22 μ F/16V
7	4	Cc0805	C15 C21 C27 C9	12 pF \pm 5%
8	8	Cc0805	C16 C22 C28 C10 C7 C5 C3 C1	39 pF \pm 5%
9	20	Rc0603	R68 R8 R10 R27 R30 R32 R49 R52 R54 R71 R74 R76 R24 R23 R5 R1 R2 R67 R46 R45	10 (**)
10	4	Rc0603	R17 R39 R61 R83	1.1k
11	8	Rc0603	R11 R33 R55 R77 R26 R48 R70 R4	2.4k
12	8	Rc0603	R6 R14 R28 R36 R50 R58 R72 R80	51
13	4	Rc0603	R89 R90 R91 R92	22
14	8	Rc0603	R15 R37 R59 R81 R21 R43 R65 R87	1.6k
15	4	Rc0603	R18 R40 R62 R84	560
16	4	Rc0603	R22 R44 R66 R88	3k
17	4	Rc0603	R25 R47 R69 R3	3.6k
18	2	Rc0603	R7 R12	"RPZ1
19	2	Rc0603	R29 R34	"RPZ2"
20	2	Rc0603	R51 R56	"RPZ3"
21	2	Rc0603	R73 R78	"RPZ4"
22	1	Rc0603	R20	"Rg1"
23	1	Rc0603	R42	"Rg2"
24	1	Rc0603	R64	" Rg3"
25	1	Rc0603	R86	" Rg4"

(*) Edge pin connectors, DIP connectors Die-Tech (LF-5104B-04-510).

(**) Tolerance of all resistors is \pm 1%.

Table B1: Component list of preshaper.

Type	R20	R42	R64	R86	R7 R12	R29 R34	R51 R56	R73 R78
1T	130	130	62	62	300	200	43	43
2T	130	130	62	62	300	300	160	43
3T	130	130	62	62	430	270	300	300
4T	130	130	62	62	360	430	270	330
5T	130	130	62	62	300	360	430	510
6T	130	130	62	62	240	270	360	390
7T	130	130	62	62	200	220	270	330
8T	130	130	62	62	160	180	240	270
9T	130	130	62	62	130	150	180	220
10T	130	130	62	62	110	130	160	180
11T	130	130	62	62	300	360	430	510
12T	130	130	62	62	200	240	300	330
13T	130	130	62	62	130	100	220	240
14T	130	130	62	62	43	43	43	91
1B	62	62	130	130	43	43	200	300
2B	62	62	130	130	43	160	300	300
3B	62	62	130	130	300	300	270	430
4B	62	62	130	130	330	270	430	360
5B	62	62	130	130	510	430	360	300
6B	62	62	130	130	390	360	270	240
7B	62	62	130	130	330	270	220	200
8B	62	62	130	130	270	240	180	160
9B	62	62	130	130	220	180	150	130
10B	62	62	130	130	180	160	130	110
11B	62	62	130	130	510	430	360	300
12B	62	62	130	130	330	300	240	200
13B	62	62	130	130	240	220	100	130
14B	62	62	130	130	91	43	43	43

Table B2: Component list of preshaper. Nominal values of the special resistors [Ω].

Appendix C: LSB output amplitudes

Fig. C1 shows the expected amplitudes of ionization signals on the LSB output. Calculations for different η towers of the HEC done for the same transverse energy $E_T = 256 \text{ GeV}$

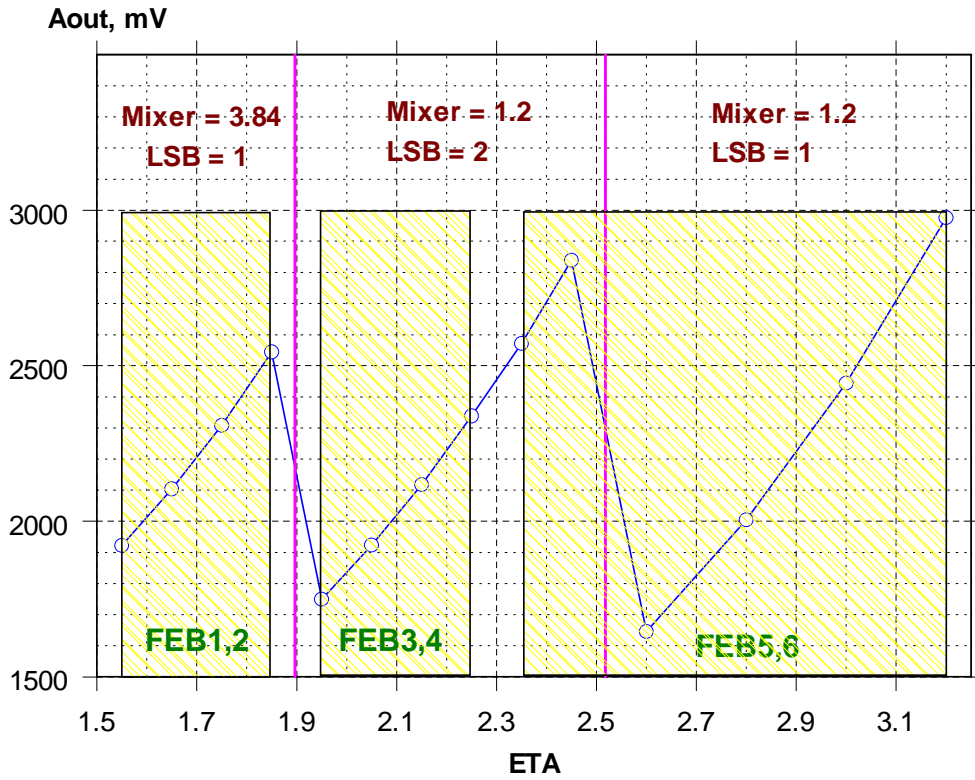


Figure C1: LSB output amplitudes for $E_T = 256 \text{ GeV}$.